Spin correlations in the algebraic spin liquid: Implications for high-T_c superconductors

Walter Rantner and Xiao-Gang Wen
Department of Physics, Massachusetts Institute of Technology, Cambridge, Massachusetts 02139
(Received 28 January 2002; revised manuscript received 10 May 2002; published 9 October 2002)

We propose that underdoped high-T_c superconductors are described by an algebraic spin liquid (ASL) at high energies, which undergoes a spin-charge recombination transition at low energies. The spin correlation in the ASL is calculated via its effective theory—a system of massless Dirac fermions coupled to a U(1) gauge field. We find that without fine-tuning any parameters the gauge interaction strongly enhances the staggered spin correlation even in the presence of a large single-particle pseudogap. This allows us to show that the ASL plus spin-charge recombination picture can explain many highly unusual properties of underdoped high-T_c superconductors.

DOI: 10.1103/PhysRevB.66.144501 PACS number(s): 74.72.−h, 75.10.−b, 76.20.+q

I. INTRODUCTION

One of the intriguing questions about the cuprate superconductors—to many possibly the key to understanding superconductivity—is the role played by spin correlations in these materials. By now it is well established that the insulating parent compound of the copper oxide superconductors is well described as a two-dimensional (2D) Heisenberg antiferromagnet (AF) in the temperature regime above the three-dimensional Néel ordering temperature ($T_N \sim 300$ K). On doping with holes, away from stoichiometry, these insulating compounds develop into high-T_c superconductors even for very low hole concentrations of the order of 5%. The question that needs to be addressed is the peculiar interplay of short-range antiferromagnetic correlations as a remnant of the ordered Neel state at zero doping competing with spin-singlet formation present in the superconducting state. The underdoped cuprates show this peculiar competition of antiferromagnetic order and singlet formation in a particularly striking way as is evidenced by various spin-pseudogaps seen in NMR and neutron scattering.

Let us briefly mention the theoretical approaches to the spin correlations in the underdoped cuprates which have emphasized the antiferromagnetic order and the concomitant spin-wave excitations as the dominant degrees of freedom. In an extensive study of the 2D antiferromagnetic Heisenberg model Chubukov, Sachdev, and Ye[1] have identified the spin correlations in the quantum critical regime at the transition from Néel order to paramagnetism. In their paper they also argue for the appearance of quantum critical scaling away from zero doping by incorporating the effect of the doped charge degrees of freedom into a reduction of the spin stiffness (finite in the ordered Néel state of the 2D Heisenberg model) Sokol and Pines[2] have similarly argued for quantum critical behavior and its crossover to a quantum-disordered regime driven by the frustration of antiferromagnetism via hole motion as the physics behind the strange spin correlations in the pseudogap regime. They postulate a susceptibility which is dominated by the effect of a finite coherence length in the quantum-disordered regime and the appearance of the corresponding *full* energy gap for spin excitations.

As we shall argue below this phenomenology qualitatively agrees with what we obtain within the slave boson approach to the *t*-*J*-model, where, however, in contrast to the above, spin-singlet formation [or, more precisely, the formation of the *d*-wave/staggered-flux phase—a state with a particular quantum order U1Cn01n (Refs. 3,4)] is the driving force behind all of the strange phenomenology in the underdoped samples.

The slave boson approach is strongly tied to the strong coupling phenomenology incorporated in the Hubbard or *t*-*J* model and was guided by Anderson's[5] exciting proposal of a spin liquid as a realization of the strongly correlated Mott insulator in the parent compound of the high-T_c superconductors. More specifically, Anderson proposed that the cuprate physics could be understood in terms of doping holes into a state which consists of preformed spin-singlet dimers on nearest-neighbor bonds whose quantum fluctuations lead to uniform strength AF correlations on all nearest-neighbor bonds [termed the resonating valence bond (RVB) state]. The RVB state has short-range antiferromagnetic spin correlations (no true long-range order) due to the singlet formation and hence comprises a spin-liquid phase. An important effect of the preformed spin singlets, present in the RVB picture, is the fact that the spin on the doped holes can become an excitation on top of the RVB collective state whereas the charge remains tied to the empty site. This led to the notion of *separate* spin and charge carrying excitations called spinons and holons, respectively. However, due to the success of the two-dimensional Heisenberg antiferromagnet in describing the insulating parent compound of the cuprates, this idea of a spin-liquid ground state was partly rejected.

Nevertheless, the RVB picture has a lot of appeal. Let us mention briefly the rationale behind the opinion that the spin-singlet formation dominates antiferromagnetic correlations in the underdoped cuprates. The slave boson approach treats the underdoped cuprates as doped Mott insulators—the key experimental fact of high-T_c superconductors. It also naturally incorporates the spin-singlet formation and predicted, ahead of experiments, the pseudogap metallic phase[6] in the underdoped cuprates and the superconducting *d*-wave order (preferred over *s*-wave order by strong Coulomb correlations present in the Mott insulator).[7] The pseudogap metallic phase is a new state of matter and it is very rare in the history of condensed matter physics that a new state of matter was predicted *before* its experimental observation.

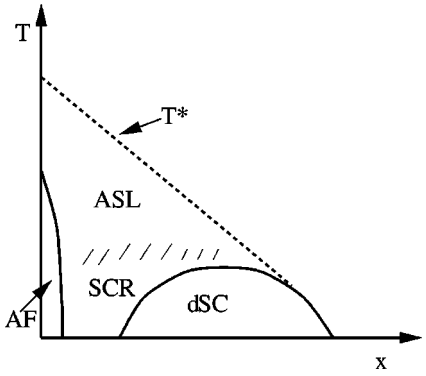

FIG. 1. Proposed phase diagram showing the ASL dominating the underdoped cuprate physics at intermediate energies and temperatures and renormalizing to an AF long-ranged state at or close to half filling and crossing over to a spin-charge recombined (SCR) phase at finite doping. T^* denotes the temperature where the crossover into the sF phase (the ASL) occurs.

However, underdoped cuprates have a very puzzling property which seems hard to explain using the spin-liquid approach (or other approaches). As the doping is lowered, both the pseudogap and AF correlation in the normal state increase. Naively, one expects the pseudogap and AF correlations to work against each other. That is, the larger the pseudogap, the stronger the spin-singlet formation, the lower the single-particle density of states, and the weaker the AF correlations.

In this paper we follow Kim and Lee[8] who considered the spin correlations in the underdoped cuprates from the perspective of incorporating gauge fluctuations on top of a particular spin-liquid state—the staggered flux (sF) phase[9] [which in turn is motivated from a mean-field treatment of the t-J model within the SU(2) slave boson approach of Wen and Lee[10]]. As Kim and Lee argued in their paper we will show explicitly how the interplay of the sF fermionic spectrum combined with massless U(1) gauge fluctuations—the effective theory of what we called the algebraic spin liquid[11] (ASL)—allows us to explain the above puzzle of strong AF correlations in the presence of a large single-particle pseudogap. Due to the U(1) gauge fluctuations present in the ASL phase, the AF spin fluctuations in the ASL are as strong as those of a nested Fermi surface, despite the pseudogap.

The main results of this paper are summarized in the phase diagram Fig. 1. At or very close to half filling, due to the enhanced AF spin fluctuations, the ASL at intermediate energies and temperatures will reorganize into a broken symmetry (long-range AF order) ground state. We show that this can happen without the need for fine-tuning a large coupling constant [this should be contrasted with random-phase-approximation (RPA) like approaches where such a fine-tuning is necessary]. In the AF state, the U(1) gauge field binds the spinons of the ASL into spin-1 spin-wave excitations.

At finite doping, the spin-charge separation physics (as embodied in the ASL) still dominates at intermediate energies and temperatures. However, in the presence of doped holes, the U(1) gauge fluctuations bind spinons and holons into electrons at low energies and temperatures. This leads to a spin-charge recombination (SCR) picture at low energies and temperatures. The ASL plus SCR at low energies allows us to give a coherent picture of the strange phenomenology of underdoped cuprates and is the main message of this paper.

In the remainder of the paper we will support the above phase diagram by performing calculations of the spin correlations in both the ASL phase and in the spin-charge recombined state.

The organization of the paper is as follows. In the next two sections (Secs. II and III) we review the ideas underlying the ASL and discuss the spin correlations in this phase outlining the calculations involved (details can be found in the Appendixes). Following this we give a brief discussion on how the recently introduced concept of quantum order[3,4] affects the current results (Sec. IV). Section V addresses the problem of what happens to the ASL physics at low energies where the interactions between spinons and holons become strong. This will be followed up by a discussion of possible implications for the cuprates and a short comparison with other approaches to the same region of the phase diagram (Sec. VI). The final section (Sec. VII) will summarize the main results and discuss open problems for further study.

II. SU(2) SLAVE BOSON APPROACH AND ALGEBRAIC SPIN LIQUID

The starting point of the slave boson approach is a microscopic lattice model. Among the popular models, the Gt-J (generalized t-J) model seems particularly promising as a description for the low doping regime where the competition between delocalization energy t and the spin fluctuations J becomes manifest:

$$H = P\sum_{(ij)}\left[J\left(\vec{S}_i\cdot\vec{S}_j-\frac{1}{4}n_in_j\right)-t(c^{\dagger}_{\alpha i}c_{\alpha j}+\text{H.c.})\right]P+\cdots. \tag{1}$$

The form of the t-J Hamiltonian can be justified starting from the Hubbard model in the limit of strong on-site Coulomb repulsion energy which in the cuprates leads to an insulating charge transfer gap of 2 eV. As the Coulomb energy is the largest energy scale in the problem it is natural to treat the kinetic energy as a perturbation which to lowest order in t^2 leads to the t-J Hamiltonian with the single-site Hilbert space restricted to the three states spin up and down and empty (indicated by the projection operator $P\cdots P$ above). For zero doping the t-J Hamiltonian reduces to the Heisenberg model with antiferromagnetic exchange coupling (virtual hopping on top of strong on-site Coulomb repulsion naturally leads to antiferromagnetic exchange).

The question of spin correlations in the cuprates ties into the question of how to reconcile local moment magnetism with itinerant electron spin density fluctuations which is a long-standing problem in condensed matter physics. There seems to be consensus in the community on how best to describe the two extreme limits of the cuprate phase diagram—the Mott insulator at zero doping as a Heisenberg antiferromagnet and the heavily doped regime in terms of itinerant electron magnetism. Of course as always the most

interesting regime is the one lying in between the two limits which shows the antiferromagnetic-singlet dichotomy described above. For the lightly doped regime one could argue that clearly a perturbation about the Néel-ordered state with frustration due to holes, in the manner of Sokol and Pines,[2] makes the most sense. However, this approach does not specify the nature of the quantum spin liquid in the disordered phase. Understanding the properties of the quantum spin liquid is very important since it is the quantum spin liquid that controls the pseudogap metallic state in the underdoped cuprates (see Fig. 1).

The (generalized) t-J-model can be shown to be an excellent description of the low-energy physics embodied in the Hubbard model under the condition that the single-site Hilbert space be constrained such that double occupation is forbidden. On an operative level this problem can be attacked by introducing slave particles that change the constraint $c_\sigma^\dagger c_\sigma(i) \leqslant 1$ [where $c_\sigma(i)$ is the physical electron destruction operator of spin σ on site i] into $\Sigma_\sigma f_\sigma^\dagger f_\sigma(i) + b^\dagger b(i) = 1$ where the $b(i)$ is a bosonic operator—the holon—that keeps track of the empty sites and carries the charge of the physical hole, whereas the spin of the hole is carried by f_σ—the fermionic spinon. This is achieved by writing $c_\sigma = f_\sigma b^\dagger$ and should be read as an equality in the constrained Hilbert space. With the introduction of the slave bosons we have, however, introduced a redundancy in the description of our physical problem which is a U(1) phase rotation of f and b that leaves the physical electron operator invariant. As the system evolves under the t-J Hamiltonian (1) this phase will strongly fluctuate as a function of space and time. It is this phase degree of freedom that corresponds to U(1) gauge fluctuations and makes the description of the constrained problem of spin + hopping in terms of fermionic and bosonic operators possible. The above program can be summarized under the name of U(1) slave boson theory and was implemented widely in the early days of high-T_c research.[12] Early on it was also realized[13] that the Heisenberg model in the fermionic representation has an extra SU(2) invariance organizing the spinons into doublets:

$$\psi_{\uparrow i} = \begin{pmatrix} f_{\uparrow i} \\ f_{\downarrow i}^\dagger \end{pmatrix}, \quad \psi_{\downarrow i} = \begin{pmatrix} f_{\downarrow i} \\ -f_{\uparrow i}^\dagger \end{pmatrix}, \tag{2}$$

In the usual U(1) slave boson approach this invariance was lost on introducing holes. More recently Wen and Lee introduced a slave boson formulation[10,14] which maintains this SU(2) structure away from half filling. This was achieved via the introduction of slave boson doublets and representing the physical electron operator as

$$c_{\uparrow i} = \frac{1}{\sqrt{2}} h_i^\dagger \psi_{\uparrow i} = \frac{1}{\sqrt{2}} (b_{1i}^\dagger f_{\uparrow i} + b_{2i}^\dagger f_{\downarrow i}^\dagger),$$
$$c_{\downarrow i} = \frac{1}{\sqrt{2}} h_i^\dagger \psi_{\downarrow i} = \frac{1}{\sqrt{2}} (b_{1i}^\dagger f_{\downarrow i} - b_{2i}^\dagger f_{\uparrow i}^\dagger), \tag{3}$$

with

$$h_i = \begin{pmatrix} b_{1i} \\ b_{2i} \end{pmatrix}$$

the doublet of bosonic fields keeping track of the doped holes.

The slave boson approach to the t-J Hamiltonian then is to use this decoupling and perform a mean-field analysis.[7,12,10] This has led to a mean-field phase diagram as a function of hole doping x and temperature T which is in qualitative agreement with the phase diagram of the cuprates. Within the mean-field description, however, the gauge freedom is treated only on the average—i.e., replaced by a static configuration of phases which in turn determine the band structure of the spinons and holons. However, as is usually the case with the identification of phases via a mean field decoupling we need to consider fluctuations about the mean-fields to determine their stability. In particular the gauge field—unconstrained by any dynamics—will affect the physical properties in each phase drastically.

In the present paper we are concerned with the pseudogap regime of the cuprates which—within the U(1) formulation—was identified as the d-wave paired state for the spinons. Within the SU(2) approach this phase can also be described as the so-called sF phase without explicit fermion pairing. As it turns out (see Ref. 14 for more details) the SU(2) formulation allows for a more straightforward identification of low-lying (massless) gauge modes and it was shown that the sF phase breaks the SU(2) gauge structure down to U(1). This massless U(1) mode was missed in the early discussions [within the U(1) slave boson approach] on the pseudogap phase and plays a crucial role in the pseudogap phase of the underdoped cuprates. It is responsible for the emergence of the ASL. In the next section we shall discuss the physical spin correlations in the ASL.

Before closing this section, we would like to remark that the ASL (the sF phase) is only one of many possible symmetric spin liquids. All symmetric spin liquids have the same symmetry, and hence we cannot distinguish different symmetric spin liquids by their symmetries. The concept of quantum order was introduced[3,4] to distinguish the different internal structures present in the symmetric spin liquids. For the symmetric spin liquids constructed within the SU(2) slave boson approach, one can use the projective symmetry group (PSG) to characterize their different quantum orders. One finds that the sF phase is described by the particular PSG with the name U1Cn01n and it is one of an infinite number of possible symmetric U(1) spin liquids. Thus the sF phase can be more accurately called U1Cn01n phase. Quantum order and its PSG characterization are very important concepts for our discussion (see Sec. IV).

III. SPIN SUSCEPTIBILITY

Our starting point is the sF (or U1Cn01n) state in the SU(2) mean-field phase diagram where the effective degrees of freedom are spinons and holons coupled to a massless U(1) gauge field. In order to analyze this problem we have mapped the lattice effective theory for the sF state (at zero doping) onto a continuum theory of massless Dirac spinors

coupled to a gauge field,[9] whose Euclidean action reads

$$S=\int d^3x\sum_{\mu}\sum_{\sigma=1}^{N}\bar{\Psi}_{\sigma}v_{\sigma,\mu}(\partial_{\mu}-ia_{\mu})\gamma_{\mu}\Psi_{\sigma}, \tag{4}$$

where $v_{\sigma,0}=1$ and $N=2$, but in the following we will treat N as an arbitrary integer. In general $v_{\sigma,1}\neq v_{\sigma,2}$. However, for simplicity we will assume $v_{\sigma,i}=1$ here. The Fermi field Ψ_{σ} is a 4×1 spinor which describes lattice spinons with momenta near $(\pm\pi/2,\pm\pi/2)$. The 4×4 γ_{μ} matrices form a representation of the Dirac algebra $\{\gamma_{\mu},\gamma_{\nu}\}=2\delta_{\mu\nu}$ $(\mu,\nu=0,1,2)$ and are taken to be

$$\gamma_0=\begin{pmatrix}\sigma_3 & 0\\ 0 & -\sigma_3\end{pmatrix},\quad \gamma_1=\begin{pmatrix}\sigma_2 & 0\\ 0 & -\sigma_2\end{pmatrix}, \tag{5}$$

$$\gamma_2=\begin{pmatrix}\sigma_1 & 0\\ 0 & -\sigma_1\end{pmatrix} \tag{6}$$

with σ_{μ} the Pauli matrices. Finally note that $\bar{\Psi}_{\sigma}\equiv\Psi_{\sigma}^{\dagger}\gamma_0$. The dynamics for the U(1) gauge field arises solely due to the screening by bosons and fermions, both of which carry gauge charge. In the low doping limit, however, we will only include the screening by the fermion fields,[8] which yields

$$\mathcal{Z}=\int Da_{\mu}\exp\left(-\frac{1}{2}\int\frac{d^3q}{(2\pi)^3}a_{\mu}(\vec{q})\Pi_{\mu\nu}a_{\nu}(-\vec{q})\right),$$

$$\Pi_{\mu\nu}=\frac{N}{8}\sqrt{\vec{q}^2}\left(\delta_{\mu\nu}-\frac{q_{\mu}q_{\nu}}{\vec{q}^2}\right). \tag{7}$$

By simple power counting we can see that the above polarization makes the gauge field a marginal perturbation at the free spinon fixed point. Importantly, however, we should note that since the conserved current (that couples to a_{μ}) cannot have any anomalous dimension, this interaction is an *exact* marginal perturbation protected by current conservation.

A. Uniform correlations

Let us now discuss how the gauge fluctuations affect spin correlations near momentum transfer $\mathbf{q}=(0,0)$. The expression for the uniform spin correlation reads (see Appendix A)

$$\langle S_u^+(x)S_u^-(0)\rangle=\int\frac{d\vec{q}}{(2\pi)^3}e^{i\vec{q}\cdot\vec{x}}\langle S_u^+(\vec{q})S_u^-(-\vec{q})\rangle,$$

$$\langle S_u^+(\vec{q})S_u^-(-\vec{q})\rangle=-\frac{1}{4}\int\frac{d\vec{p}}{(2\pi)^3}\mathrm{Tr}[\gamma_0G(\vec{p})\gamma_0G(\vec{p}-\vec{q})], \tag{8}$$

where $\langle\cdots\rangle$ denotes the expectation value with respect to theory (4). From this expression we see that the uniform spin correlation is proportional to Π_{00}, the polarization operator of the spinons. Hence it cannot be strongly affected by the massless gauge field as we argued above via current conservation. This was shown in an explicit calculation by Chen, Fisher, and Wu in the context of the fractional quantum Hall (FQH) effect.[15] Contrasting to this as was suggested by Kim and Lee[8] we would expect the gauge fluctuations to strongly affect the staggered spin correlations which are not protected by current conservation and restore antiferromagnetic correlations[16] which have been largely lost in the mean-field singlet state as we shall see next.

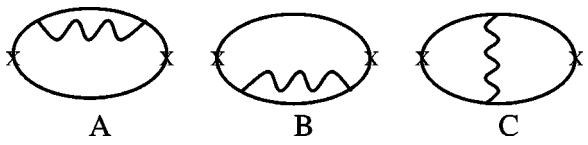

FIG. 2. Nonzero leading $1/N$ corrections to the staggered spin correlation function. The $\times$ denotes the vertex which is the 4×4 unit matrix in the case of interest.

B. Staggered correlations

In the following we will present fluctuation corrections to the antiferromagnetic spin-spin correlations at order $1/N$. The expression for the staggered correlation is obtained in the form (see Appendix A)

$$\langle S_s^+(\vec{q})S_s^-(-\vec{q})\rangle=-\frac{1}{4}\int\frac{d\vec{p}}{(2\pi)^3}\mathrm{Tr}[\mathbb{1}G(\vec{p})\mathbb{1}G(\vec{p}-\vec{q})]. \tag{9}$$

At the mean-field level this is simply

$$\langle S_s^+(\vec{q})S_s^-(-\vec{q})\rangle_0=-\frac{1}{4}\int\frac{d\vec{p}}{(2\pi)^3}\mathrm{Tr}[\mathbb{1}G_0(\vec{p})\mathbb{1}G_0(\vec{p}-\vec{q})],$$

where $G_0(\vec{p})=-i/p_{\mu}\gamma^{\mu}$ and the vertices are the 4×4 unit matrices denoted $\mathbb{1}$. Decoupling the denominator in the usual way via Feynman parameters we obtain

$$\langle S_s^+(\vec{q})S_s^-(\vec{q})\rangle_0=-\frac{\sqrt{q_0^2+\mathbf{q}^2}}{16}. \tag{10}$$

Note that $\mathbf{q}$ is measured with respect to (π,π) in units of the lattice spacing. From expression (10), we see that the antiferromagnetic correlations have been largely lost. The reason for this can be traced back to the spin-singlet formation in the mean-field sF (U1Cn01n) phase. This motivates the inclusion of gauge fluctuations. At order $1/N$ we have the three nonvanishing diagrams depicted in Fig. 2. In order to calculate the contribution of these diagrams we note that unlike the single-spinon spectral function the density-density correlation is gauge invariant and hence we can choose to work in the Landau gauge where the gauge propagator reads

$$D_{\mu\nu}(\vec{q})=\frac{8}{N\sqrt{\vec{q}^2}}\left(\delta_{\mu\nu}-\frac{q_{\mu}q_{\nu}}{\vec{q}^2}\right) \tag{11}$$

and we have the following expressions for the diagrams shown:

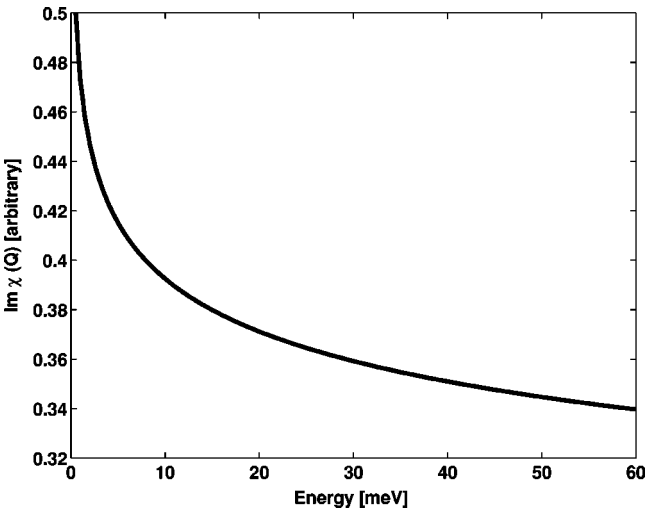

FIG. 3. Imaginary part of the spin susceptibility at $\mathbf{Q}_{\mathrm{AF}}$. Note the divergence at small ω.

$$[2(\mathrm{A})]+[2(\mathrm{B})]=-\frac{1}{2}\int\frac{d^dk}{(2\pi)^d}\int\frac{d^dq}{(2\pi)^d}\times\mathrm{Tr}\left[\mathbb{1}\frac{1}{i(p+k)_\epsilon\gamma^\epsilon}\mathbb{1}\frac{1}{ik_\delta\gamma^\delta}i\gamma^\mu D_{\mu\nu}(\vec{q})\times\frac{1}{i(k+q)_\beta\gamma^\beta}i\gamma^\nu\frac{1}{ik_\alpha\gamma^\alpha}\right],\tag{12}$$

$$[2(\mathrm{C})]=-\frac{1}{4}\int\frac{d^dk}{(2\pi)^d}\int\frac{d^dq}{(2\pi)^d}\times\mathrm{Tr}\left[\mathbb{1}\frac{1}{i(p+k)_\epsilon\gamma^\epsilon}i\gamma^\mu\frac{1}{i(p+k+q)_\delta\gamma^\delta}\times\mathbb{1}\frac{1}{i(k+q)_\beta\gamma^\beta}i\gamma^\nu\frac{1}{ik_\alpha\gamma^\alpha}D_{\mu\nu}(\vec{q})\right].\tag{13}$$

After performing the trace and integrating over k in $d=3$, where the integrals are convergent (see Appendix B), we arrive at

$$[2(\mathrm{A})]+[2(\mathrm{B})]=\frac{1}{N}\int\frac{d^dq}{(2\pi)^d}\left[\frac{2\vec{p}\cdot\vec{q}+\vec{p}^2}{|\vec{q}|^3|\vec{p}+\vec{q}|}-\frac{\vec{p}\cdot\vec{q}}{|\vec{p}|\vec{q}^2|\vec{p}+\vec{q}|}-\frac{|\vec{p}|}{|\vec{q}|^3}\right],\tag{14}$$

$$[2(\mathrm{C})]=\frac{1}{N}\int\frac{d^dq}{(2\pi)^d}\left[\frac{2}{\vec{q}^2}+\frac{|\vec{p}|}{|\vec{q}|^3}-\frac{\vec{p}^2+2\vec{p}\cdot\vec{q}}{|\vec{q}|^3|\vec{p}+\vec{q}|}-\frac{4|\vec{p}|}{\vec{q}^2|\vec{p}+\vec{q}|}-\frac{\vec{q}^2\vec{p}^2+2\vec{p}^4}{\vec{p}\cdot\vec{q}\vec{q}^2|\vec{p}||\vec{p}+\vec{q}|}\right].\tag{15}$$

In order to proceed we need to regularize the above integrals. Because of the dot product appearing in the denominator of the last term in Eq. (15), it is hard to use dimensional regularization. Hence we have set $d=3$ and introduced an upper momentum cutoff Λ. Thus performing the final integrals over $\vec{q}$ we can extract the log-divergent term in the form

$$[2(\mathrm{A})]+[2(\mathrm{B})]+[2(\mathrm{C})]=-\frac{8}{12\pi^2N}|\vec{p}|\ln\left(\frac{\Lambda^2}{\vec{p}^2}\right).$$

After combining this with the mean-field result (10) and continuing to real frequencies (see Appendix B) we obtain

$$\begin{aligned}\mathrm{Im}\chi(\omega,\mathbf{q})&\equiv\chi''(\omega,\mathbf{q})\\&\equiv\mathrm{Im}\langle S_s^+(\omega,\mathbf{q})S_s^-(-\omega,-\mathbf{q})\rangle\\&=C_s\frac{1}{2}\sin(2\nu\pi)\Gamma(2\nu-2)\\&\quad\times\Theta(\omega^2-\mathbf{q}^2)(\omega^2-\mathbf{q}^2)^{1/2-\nu},\\\nu&=\frac{32}{3\pi^2N},\end{aligned}\tag{16}$$

where C_s is a constant depending on the physics at the lattice scale. In the limit $N\to\infty$ this reduces to the mean-field result (10).

From Eqs. (16) it is clear that the gauge fluctuations have reduced the mean-field exponent. If we boldly set $N=2$, which is the physically relevant case, we find $\nu>1/2$, signaling an antiferromagnetic instability. This value of ν is consistent with an earlier numerical result obtained in Ref. 16. Ivanov *et al.* employing a Gutzwiller projection found that for the case of small hole doping of order 5% the staggered spin correlation decays in real space as $r^{-2.4}$ which corresponds to a change from the mean-field exponent $\propto r^{-4}$ by $+1.6$. Our calculation in turn yields an increase in the real space exponent from -4 to -2.92 a change by $+1.08$. Furthermore, our result agrees with the first-order term in the $1/N$ expansion of the nonperturbative result obtained in the context of spontaneous chiral symmetry breaking in Ref. 17. Expanding their result to $1/N^2$ allows us to at least estimate the sign and order of magnitude that higher-order corrections will play and shows in effect that $1/N^2$ corrections have the appropriate sign to increase the real space exponent even further, bringing the analytic result closer in line with the exact numerical data. In Fig. 3 we plot the imaginary part of the spin susceptibility at $\mathbf{q}=0\equiv\mathbf{Q}_{\mathrm{AF}}=(\pi,\pi)$. Let us also remark that although we do not know the exact value of ν, many results discussed in this paper remain valid since they are not sensitive to the value of ν. Those results mainly depend on two things: (A) ν is close to or bigger than 1/2, a large change from the mean-field exponent, and (B) ν is irrational. Condition (B) ensures a branch cut in the spin-spin correlation function, which is needed to explain experimental data.

This result is quite natural in the light of what has been said so far. The gauge fluctuations arise from the constraint

of no double occupancy. The dynamics for the gauge field—in the very low doping limit assumed here—is solely due to virtual spinons. It is the low energy spinon-antispinon pairs having a nesting condition for scattering between the nodes (separated by $\mathbf{Q}_{\mathrm{AF}}$) in the sF (U1Cn01n) phase mean-field spectrum which are responsible for the antiferromagnetic enhancement in the ASL phase. Let us emphasize again that this enhancement of spin correlations at $\mathbf{Q}_{\mathrm{AF}}=(\pi,\pi)$ over the uniform component is protected, just like the gapless U(1) gauge fluctuations and the gapless spinons, by the U1Cn01n quantum order

We have thus established algebraic behavior for the staggered spin correlations. It is such an algebraic correlation that leads to the name ASL that we assigned to the phase.

C. Correlations near $(\pi,0)$

For this momentum transfer the spinons get scattered between the two different types of nodes in the sF spectrum which yields the following expression for the corresponding correlations

$$\langle S^{+}_{(\pi,0)}(\vec{q})S^{-}_{(\pi,0)}(-\vec{q})\rangle = -\frac{1}{4}\int \frac{d\vec{p}}{(2\pi)^3}\mathrm{Tr}\left[\begin{pmatrix}0 & \sigma_1\\ \sigma_1 & 0\end{pmatrix} \times G(\vec{p})\begin{pmatrix}0 & \sigma_1\\ \sigma_1 & 0\end{pmatrix}G(\vec{p}-\vec{q})\right]. \tag{17}$$

Having worked hard to obtain the anomalous dimension of the staggered spin operator by brute force we will here resort to standard field theory renormalization apparatus which allows for a more economical derivation of the anomalous dimensions of composite operators. In order to obtain the anomalous dimension of the spin operator which is a fermion bilinear we need to obtain its wave function renormalization in the form

$$Z_S = Z_\Psi Z_\Gamma, \tag{18}$$

where Γ is the relevant vertex and as we have seen above depends on the momentum transfer, that is,

$$\Gamma = \gamma_0, \mathbb{1}, \begin{pmatrix}0 & \sigma_1\\ \sigma_1 & 0\end{pmatrix}$$

near $(0,0),(\pi,\pi)$, and $(\pi,0)$, respectively.

The spinon wave function renormalization is obtained from the self-energy in the usual way and evaluates in the Landau gauge to

$$Z_\Psi = 1+\frac{4}{N}\frac{1}{3\pi^2}\frac{\Gamma\left(\frac{3-d}{2}\right)}{(M^2)^{(3-d)/2}}, \tag{19}$$

where M is the renormalization scale and we have used dimensional regularization.

To obtain the vertex renormalization we need to evaluate the divergent part of the one-loop diagram depicted in Fig. 4

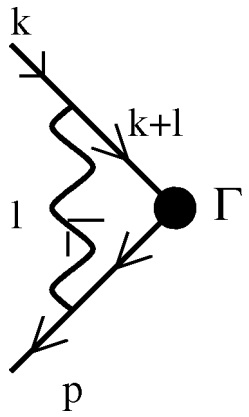

FIG. 4. Fermion-fermion vertex.

which reads

$$\int \frac{d^3l}{(2\pi)^3}\frac{i\gamma^\mu(-i\gamma^\epsilon)(k+l)_\epsilon\Gamma(-i\gamma^\delta)(l+p)_\delta i\gamma^\nu D_{\mu\nu}(l)}{(k+l)^2(p+l)^2},$$

where Γ is the relevant vertex and $D_{\mu\nu}$ is given by Eq. (11). Since the vertex correction diverges only logarithmically, we can simply evaluate the divergent part by setting all the incoming momenta equal to 0. Hence the above simplifies to

$$\frac{8}{N}\int \frac{d^dl}{(2\pi)^d}\left[\frac{\gamma^\mu l_\epsilon\gamma^\epsilon\Gamma_{(\pi,0)}l_\delta\gamma^\delta\gamma^\nu\delta_{\mu\nu}}{l^5} - \frac{\gamma^\mu l_\epsilon\gamma^\epsilon\Gamma_{(\pi,0)}l_\delta\gamma^\delta\gamma^\nu l_\mu l_\nu}{l^7}\right],$$

where we now concentrate on the $(\pi,0)$ vertex.

This can be easily evaluated with the help of

$$\gamma_\epsilon\Gamma_{(\pi,0)} = (1-2\delta_{\epsilon 2})\Gamma_{(\pi,0)}\gamma_\epsilon\int \frac{d^dl}{(2\pi)^d}\frac{1}{l^3}\Big|_{div} = \frac{1}{4\pi^2}\frac{2}{3-d}$$

and results in

$$Z_{\Gamma_{(\pi,0)}} = 1-\frac{4}{N}\frac{1}{3\pi^2}\frac{\Gamma\left(\frac{3-d}{2}\right)}{(M^2)^{(3-d)/2}}, \tag{20}$$

which together with Eqs. (18) and (19) gives

$$Z_{S_{(\pi,0)}} = 1. \tag{21}$$

Hence the spin operator at $(\pi,0)$ does not pick up any anomalous dimension from the gauge field interactions. It is not hard to check within the above-outlined calculation that for the other two vertices corresponding to the uniform and staggered spin operators, we recover the results discussed in the previous sections which gives a nice check on the brute force calculation.

IV. PERTURBATIVE STABILITY OF THE sF (U1Cn01n) PHASE

An important technical detail was hidden in the above calculation. In this section, we will expose this issue.

The sF phase contains two families of four-component massless Dirac fermions, which couple to massless U(1) gauge fluctuations. At the perturbative level, the interaction can generate many possible counterterms (in this case the self-energy terms) which can (A) generate a mass for the Dirac fermions, (B) generate a finite chemical potential for the Dirac fermions and change the Fermi points into Fermi pockets, and (C) shift the crystal momenta of the Dirac fermions from $(\pm\pi/2,\pm\pi/2)$ to some other values. In our perturbative calculation in the last section, we have assumed that none of the above counterterms are generated by the interaction.

In a generic interacting theory, we used to believe that all the counterterms that are consistent with symmetries will be generated. All of the above three types of counterterms are consistent with the underlying lattice symmetries and are hence allowed by the symmetries. In fact they do appear in our calculation of the continuum theory as cutoff-dependent terms. It appears that the results in the last section are incorrect since the important counterterms are ignored. Those counter terms, if present, will drastically alter our previous results.

As was stressed in this paper and in Refs. 3 and 4, the sF phase, as a quantum spin liquid, is not only characterized by its symmetry but also by its quantum order. The quantum order in the sF phase is characterized by a particular PSG: U1Cn01n. The mean-field ansatz of the sF phase is invariant under the transformations of the U1Cn01n PSG. As pointed out in Refs. 3 and 4, the perturbative fluctuations around the mean-field ground state may deform the mean-field ansatz. Those deformations correspond to the counterterms. However, in our case, it is incorrect to use symmetries to determine which counterterms are allowed. One should use the PSG to determine the allowed counterterms. This is because perturbative fluctuations can only deform the ansatz in such a way that the deformed ansatz remains invariant under the same PSG. It was shown[4] that the above three counterterms are forbidden by the U1Cn01n PSG. This is why we can drop them in our calculation.

When we calculate the effects of interactions in a continuum theory, we introduce a high-energy short-distance cutoff. This cutoff destroys the structure of the underlying quantum order. Thus it is not surprising that the counterterms forbidden by the quantum order show up in continuum theory as cutoff-dependent terms. To restore the quantum order that existed in the underlying lattice theory, we can simply drop all the forbidden counterterms in our calculation within the continuum theory. We see that the PSG and the concept of quantum order play an important role even in calculations within continuum theories. It is the understanding of the PSG and quantum order that makes sensible calculations in the continuum limit possible. In fact, the theory of quantum order is partly motivated by the above issue of the counterterms.

In summary, the perturbative fluctuations around the mean-field sF (U1Cn01n) state cannot change the quantum order and cannot generate energy gaps for the U(1) gauge field and the spinons.[4] Thus the gapless U(1) gauge fluctuations and the gapless spinons are protected by the U1Cn01n quantum order present in the sF (U1Cn01n) phase. They remain gapless even when the interaction is finite all the way down to zero energy. The interacting gapless excitations lead to many unusual properties of underdoped cuprates, such as the non-Fermi liquid behavior of the normal metallic state, the broad electron spectral function[11], and the diverging AF spin fluctuations in the presence of the pseudogap. The U1Cn01n quantum order in the sF phase not only protects the gapless excitations; it also protects the momentum of the gapless excitations. For example, the spin-1 gapless excitations can only appear near $\mathbf{k}=(0,0)$, (π,π), $(0,\pi)$, and $(\pi,0)$.

We would like to point out that although the ASL can be a stable quantum phase in the large N limit,[18,4] for the real $N=2$ case, nonperturbative instanton effects cause an instability. Thus at low energies the ASL will change into some other state, such as the *d*-wave superconducting state, the AF state, stripe states, or even a Z_2 spin-liquid state. Since the U1Cn01n quantum order in the sF phase requires the spin-1 gapless excitations to appear at $\mathbf{k}=(0,0),(\pi,\pi),(\pi,0),(0,\pi)$, the shift of the low-frequency neutron scattering peak observed in experiments[19–25] indicates a transition from the ASL to some other state at low temperatures. Studying how the momentum of spin-1 gapless excitations shifts away from (π,π), $(\pi,0)$, and $(0,\pi)$ will allow us to experimentally identify the low-temperature phase. In the last section, we have studied the spin fluctuations in the ASL. In the following section, we will study the spin fluctuations in the low-temperature phase.

V. THE FATE OF THE ASL

In Sec. III, we showed how the ASL physics reconciles the pseudogap formation (i.e., the condensation into spin singlets within the RVB picture) with enhanced dynamical antiferromagnetic fluctuations. At lower energies the ASL is unstable—and an important question is how the ASL evolves in the underdoped regime into the superconducting state as we reduce temperature.

In the following we are going to address this question via first analyzing the effect of the opening of a gap in the gauge fluctuations on the staggered spin correlations. Intuitively we should expect that for energies below the mass gap the spin correlations should be given by mean-field correlations—which is indeed the case. Having established the profound effects of this gap formation we take a more careful look at the change of the mean-field correlations on going from the sF (U1Cn01n) phase into the fermion pairing state which will allow us to address the question of incommensurate spin fluctuations seen at low frequencies and temperatures in the cuprates. Let us now proceed to consider the effect of giving a mass to the gauge fluctuations. In the context of the spin correlations considered here, we would thus expect the destruction of the antiferromagnetic enhancement below the

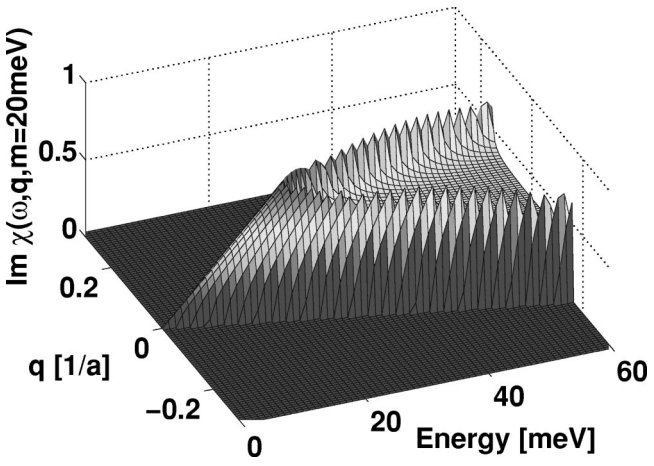

FIG. 5. Scan of the imaginary part of the spin susceptibility in arbitrary units for $\mathbf{q}=-\pi/10-\pi/10$ and $\omega=0-60$ meV. We have chosen $m=20$ meV in this plot.

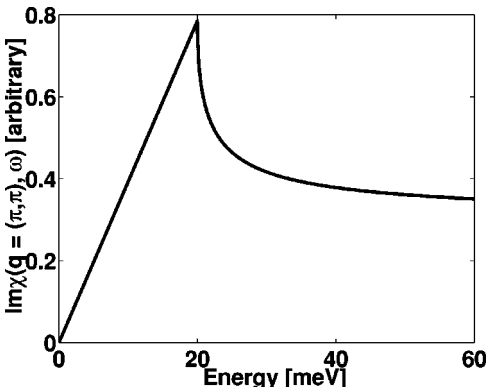

FIG. 6. Imaginary part of the spin susceptibility at $\mathbf{Q}_{\mathrm{AF}}$ where $m=20$ meV notice the recovery of the linear mean-field result below the mass gap.

mass gap and a resurfacing of the singlet character of the correlations in the mean-field sF (U1Cn01n) phase.

To implement the mass gap formation we take the following phenomenological form for the gauge propagator:[11]

$$D_{\mu\nu}(\vec{q})=\frac{8}{N\sqrt{\vec{q}^2+m^2}}\left(\delta_{\mu\nu}-\frac{q_\mu q_\nu}{\vec{q}^2}\right).$$

The calculation then goes through as above (with one subtlety in the analytic continuation discussed in the Appendix B) resulting in the following expression for the staggered correlation

$$\begin{aligned}&\mathrm{Im}\langle S_s^+(\omega,\mathbf{q})S_s^-(\omega,\mathbf{q})\rangle\\&\quad=\Theta(\omega^2-\mathbf{q}^2)\Theta[m^2+\mathbf{q}^2-\omega^2)]C_m\frac{\sqrt{\omega^2-\mathbf{q}^2}}{m^{2\nu}}\\&\quad+\Theta[\omega^2-\mathbf{q}^2-m^2]\\&\quad\times C_m\frac{\sqrt{\omega^2-\mathbf{q}^2}}{(\sqrt{\omega^2-\mathbf{q}^2}+\sqrt{\omega^2-\mathbf{q}^2-m^2})^{2\nu}},\end{aligned}\tag{22}$$

where

$$\nu=\frac{32}{3\pi^2N}.$$

In Fig. 5 we plot a momentum scan of the resulting spectra with $m=20$ meV. Figure 6 depicts the spectrum at the antiferromagnetic ordering wavevector $\mathbf{Q}_{\mathrm{AF}}$. As expected the opening of the mass gap in the gauge fluctuations has restored the mean-field result and consequently suppressed the antiferromagnetic enhancement seen in Fig. 3.

From this analysis we see that the spin correlations at low frequencies are described by the underlying mean field. In the above calculation we have assumed that the only effect of the destruction of the massless U(1) gauge structure in the sF phase is the formation of the U(1) mass gap which leaves the underlying mean-field correlations in tact at low energies. On a more profound level, however, the massless nature of the U(1) gauge structure in the sF state is a manifestation of the U1Cn01n quantum order[4] present in this state (see the Introduction and Sec. IV). Thus it is not possible to simply break the gauge structure without affecting the underlying mean-field ansatz as we have assumed above. If we reverse the above logic, this implies that the low-frequency spin correlations which reflect the underlying mean-field ansatz can be used as an experimental probe into the corresponding quantum order and gauge structure accompanying the mean-field correlations.

The ASL described by the sF (U1Cn01n) state may change into several different states at low temperatures. The low energy spin correlation can have different behaviors in those low-temperature states. In the following, we will discuss one particular low-temperature state to gain some intuition on the behavior of the low-energy spin correlation in the low temperature phases.

Within the SU(2) slave boson theory, the mean-field phase which is energetically favored over the sF (U1C01n) phase at low temperatures is the so-called *d*-wave pairing state.[14] In order to keep this section reasonably self-contained we would like to outline some of the steps leading to the mean-field correlations discussed in the following. As was mentioned above within the SU(2) slave boson formulation the physical electron operator is represented as

$$\begin{aligned}c_{\uparrow i}&=\frac{1}{\sqrt{2}}h_i^\dagger\psi_{\uparrow i}=\frac{1}{\sqrt{2}}(b_{1i}^\dagger f_{\uparrow i}+b_{2i}^\dagger f_{\downarrow i}^\dagger),\\c_{\downarrow i}&=\frac{1}{\sqrt{2}}h_i^\dagger\psi_{\downarrow i}=\frac{1}{\sqrt{2}}(b_{1i}^\dagger f_{\downarrow i}-b_{2i}^\dagger f_{\uparrow i}^\dagger),\end{aligned}\tag{23}$$

where the following SU(2) doublets were introduced:

$$\psi_{\uparrow i}=\begin{pmatrix}f_{\uparrow i}\\f_{\downarrow i}^\dagger\end{pmatrix},\quad\psi_{\downarrow i}=\begin{pmatrix}f_{\downarrow i}\\-f_{\uparrow i}^\dagger\end{pmatrix},\quad h_i=\begin{pmatrix}b_{1i}\\b_{2i}\end{pmatrix}.$$

The $\psi_{\uparrow i}$ and $\psi_{\downarrow i}$ are the two fermion fields representing the destruction of a spin up and spin down on site i, respectively, and h_i is the doublet of bosonic fields keeping track of the doped holes. Putting this representation into the t-J Hamiltonian

$$H = P \sum_{(ij)} \left[J\left(\vec{S}_i \cdot \vec{S}_j - \frac{1}{4} n_i n_j \right) - t(c^{\dagger}_{\sigma i} c_{\sigma j} + \text{H.c.}) \right] P$$

yields on performing a Hubbard-Stratonovich transformation to the appropriate bosonic bond variables the following partition function:[14]

$$Z = \int DhDh^{\dagger} D\psi^{\dagger} D\psi D\vec{a}_0 DU \exp\left(- \int_0^{\beta} L \right), \quad (24)$$

$$\begin{aligned} L = & \frac{\tilde{J}}{2} \sum_{\langle ij \rangle} \mathrm{Tr}[U^{\dagger}_{ij} U_{ij}] + \frac{1}{2} \sum_{i,j,\sigma} \psi^{\dagger}_{\sigma i} (\partial_{\tau} \delta_{ij} + \tilde{J} U_{ij}) \psi_{\sigma j} \\ & + \sum_{il} a^{l}_{0i} \left(\frac{1}{2} \psi^{\dagger}_{\sigma i} \tau^{l} \psi_{\sigma i} + h^{\dagger}_{i} \tau^{l} h_i \right) + \sum_{ij} h^{\dagger}_{i} [(\partial_{\tau} - \mu) \delta_{ij} \\ & + \tilde{t} U_{ij}] h_j . \end{aligned} \quad (25)$$

The $\vec{a}_0$ fluctuations incorporate the projection to the space of SU(2) singlets within the above representation for the electron operators (23). Furthermore, note that[26] $\tilde{J} = 3J/8$, $\tilde{t} = t/2$ and the matrix U_{ij} in the form

$$U_{ij} = \begin{pmatrix} -\chi^{*}_{ij} & \Delta_{ij} \\ \Delta^{*}_{ij} & \chi_{ij} \end{pmatrix}$$

contains the Hubbard-Stratonovich fields which classify the part of the phase diagram we are looking at. The mean-field phase diagram is found by minimizing the free energy for a given number of particles with respect to the bond variables U_{ij}.

The d-wave pairing state can be represented as

$$\begin{aligned} U_{i,i+\hat{x}} &= -\tau^3 \chi + \tau^1 \Delta, \\ U_{i,i+\hat{y}} &= -\tau^3 \chi - \tau^1 \Delta, \\ a^3_0 &\neq 0. \end{aligned} \quad (26)$$

The key difference to the sF (U1Cn01n) phase is the appearance of a finite a^3_0 which acts as a chemical potential for the spinons. Without this term the above ansatz is SU(2)-gauge equivalent to the sF (U1Cn01n) ansatz.[14] It is shown in Ref. 4 that the appearance of such a chemical potential term is not consistent with the quantum order of the sF (U1Cn01n) phase and hence signals the presence of a different quantum order accompanying the d-wave pairing state. It is precisely a nonzero a^3_0 which gives rise to an anomalous fermion-fermion pairing which when combined with holon condensation leads to the d-wave superconducting state. As we shall see in the following, a^3_0 is also responsible for the incommensurate spin response at the lowest frequencies shifting the peak away from $\mathbf{Q}_{\mathrm{AF}} = (\pi, \pi)$.

Taking the above ansatz equation (26) we can calculate the spin-spin correlations at mean-field level (see Appendix E) to obtain for the imaginary part of the spin correlation near $\mathbf{Q}_{\mathrm{AF}} = (\pi, \pi)$:

$$\begin{aligned} & \mathrm{Im}\langle S^{+}(\omega, \mathbf{Q}_{\mathrm{AF}} + \mathbf{k}) S^{-}(-\omega, -\mathbf{Q}_{\mathrm{AF}} - \mathbf{k}) \rangle \\ & = \frac{1}{64 v_f v_2} \{ \theta[\omega^2 - (v_f k_1 + 2a^3_0)^2 - v^2_2 k^2_2] \sqrt{\omega^2 - (v_f k_1 + 2a^3_0)^2 - v^2_2 k^2_2} + \theta[\omega^2 - (v_f k_1 - 2a^3_0)^2 - v^2_2 k^2_2] \\ & \quad \times \sqrt{\omega^2 - (v_f k_1 - 2a^3_0)^2 - v^2_2 k^2_2} + \theta[\omega^2 - (v_f k_2 + 2a^3_0)^2 - v^2_2 k^2_1] \sqrt{\omega^2 - (v_f k_2 + 2a^3_0)^2 - v^2_2 k^2_1} \\ & + \theta[\omega^2 - (v_f k_2 - 2a^3_0)^2 - v^2_2 k^2_1] \sqrt{\omega^2 - (v_f k_2 - 2a^3_0)^2 - v^2_2 k^2_1} \}, \end{aligned}$$

$$k_1 \equiv \frac{k_x + k_y}{\sqrt{2}} \quad k_2 \equiv \frac{-k_x + k_y}{\sqrt{2}} \quad v_f \equiv 2\sqrt{2} a J \chi \quad v_2 \equiv 2\sqrt{2} a J \Delta. \quad (27)$$

In Fig. 7 we plot the resulting spectrum for a frequency $\omega < \omega_c \equiv (4/\sqrt{3})(v_2/v_f) a^3_0$ where the intensity is peaked around four points shifted diagonally away from $\mathbf{Q}_{\mathrm{AF}}$. In contrast to this in Fig. 8 we depict a scan for $\omega > \omega_c$ the spectrum is peaked at four points shifted horizontally $(\pi \pm \delta, \pi), (\pi, \pi \pm \delta)$ where the ridges—growing out perpendicular to the diagonals—overlap. δ is related to a^3_0 via $\delta a = a^3_0 / J$ with a the lattice spacing. It should be noted that in the $\omega \to 0$ the peaks are always located along the diagonal, as expected, for in this regime the response is dominated by creation of particle-hole pairs connecting the Fermi points. Interestingly for intermediate energies the peak intensity in the spectrum is shifted *horizontally* away from $\mathbf{Q}_{\mathrm{AF}}$ even without one-dimensional phenomenology.

VI. APPLICATION TO HIGH-T_c

Before launching into a discussion of how the above-mentioned physics embodied in the ASL might shed some

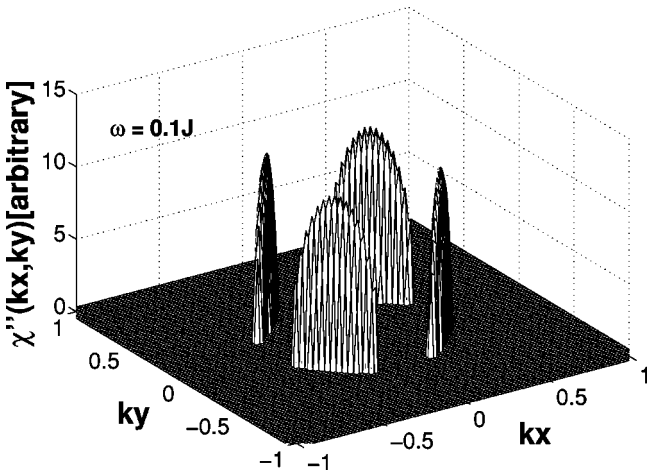

FIG. 7. Wave vector scan of $\chi''(k_x,k_y,\omega=0.1J)$. Notice the incommensurate pattern at low energy with amplitude peaks shifted along the diagonals (Ref. 27). (0,0) corresponds to $\mathbf{Q}_{\mathrm{AF}}$ and k_x,k_y are measured in units of $1/a$ with a the lattice spacing.

light on the cuprate spin physics we need to briefly digress and establish some nomenclature. As we shall see in the following each experimental community has their own set of pseudo gaps and spin pseudogaps and it is easy to get lost in the confusing terminology. Here we adopt the following convention.

Pseudogap phase denotes the part in the cuprate phase diagram where angle-resolved photoemission experiments observe a large gap in the single-particle spectrum at $(\pi,0)$.

The term *spin pseudogap* will be used in conjunction with the spectrum at the antiferromagnetic wave vector $\mathbf{Q}_{\mathrm{AF}}=(\pi,\pi)$ to denote the frequency range of reduced spectral weight below the peak above T_c (which on cooling below T_c shifts to higher frequencies and becomes the ''resonance''—see discussion below).

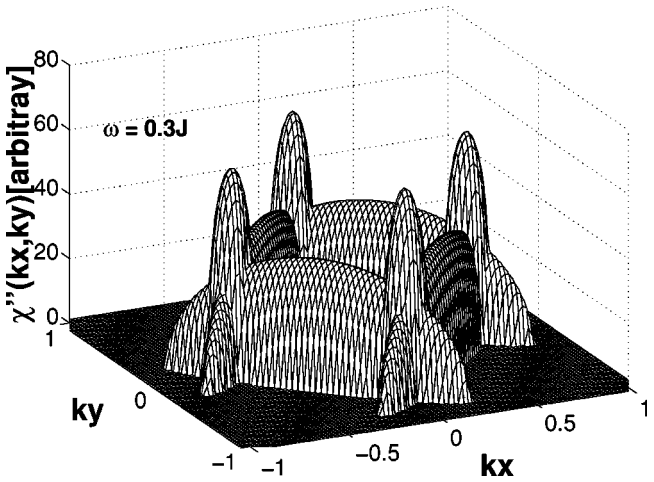

FIG. 8. Wave vector scan of $\chi''(k_x,k_y,\omega=0.1J)$, k_x,k_y are measured in units of $1/a$. With a_0^3 chosen to give $\delta a=0.1$ r.l.u. $(2\pi=1$ r.l.u.) (Refs. 28 and 29) the value of ω_c is set by $\omega_c=(4/\sqrt{3})(v_2/v_f)\delta a J$. To compare with experiments we have chosen the values $v_2/v_f=1/7$ (Ref. 30), which gives $\omega_c=0.2J$. Notice how the overlapping ridges lead to the horizontal incommensuration.

Over the years NMR and inelastic neutron scattering (INS) have painted a very interesting picture for the spin correlations in the cuprates starting with the discovery of the by now famous 41 meV ''resonance'' peak by Rossat-Mignod *et al.*[31] in the superconducting state of near-optimally doped $YBa_2Cu_3O_7$. In addition to this resonance mode which appears exclusively in the superconducting state there is now evidence for a precursory piling up of spectral weight in the energy region of the ''resonance'' even in the normal state of underdoped cuprates. The energy at which this enhancement occurs in the normal state is sometimes referred to as the ''spin-pseudogap'' energy by INS workers[32] (hence our convention). From the perspective of spin fluctuations INS is clearly the most powerful probe, giving both dynamical and wave-vector-dependent information about the spectrum.

NMR, on the other hand, probes particular regions in wave vector space with Knight shift probing the uniform susceptibility—$\propto\chi(\mathbf{q}=0,\omega\sim0)$—and spin-lattice relaxation rate probing $\sim\mathrm{Im}\chi(\mathbf{q}_{C_u,O},\omega)/\omega|_{\omega\to0}$ where $\mathbf{q}_{C_u}=\mathbf{Q}_{\mathrm{AF}}$ and $\mathbf{q}_O=\mathbf{0}$ are the characteristic wave vectors determining the spin-lattice relaxation at the planar C_u and O sites, respectively. In addition to the above-mentioned ''spin pseudogap,'' NMR has identified two characteristic temperatures. One is the reduction of the Knight shift below a temperature which we will denote by T_N which indicates the loss of spectrum for $\chi(\mathbf{q}=0,\omega\sim0)$ below this characteristic temperature. Furthermore, there is a second *lower* scale which shows up in the spin-lattice relaxation rate for C_u as a peak in $(1/T_1T)$ which we shall call T_{T_1}. Notice that $T_{T_1}<T_N$ but both of these temperatures are above the superconducting transition temperature T_c in underdoped samples. From the perspective of mean-field theory it is impossible to explain these observations.[33] Within the mean-field picture the reduction of the Knight shift below T_N can be related to the reduction of spin fluctuations on condensing into the spin-singlet sector identified as the sF (U1Cn01n) phase above. However, there is then no way to explain the difference in the spin-lattice relaxation rates observed for planar C_u and O. Whereas $(1/T_1T)_{C_u}$ increases with decreasing temperature between $T_N>T>T_{T_1}$, $(1/T_1T)_O$ reduces monotonically below T_N.

Let us now discuss these interesting phenomena from the point of view of the ASL physics described in the previous part. As has been suggested by Kim and Lee[8] the enhancement of C_u over O relaxations is expected to depend on the inclusion of the gauge fluctuations. The rational for this suggestion arises from the fact that C_u-NMR probes $\mathbf{q}\sim\mathbf{Q}_{\mathrm{AF}}$ fluctuations which are strongly affected by the gauge fluctuations whereas O-NMR derives its main contributions from $\mathbf{q}\sim\mathbf{0}$ which is protected from gauge fluctuations by current conservation. We have shown above that this enhancement indeed takes place with $\mathrm{Im}\chi_{\mathbf{Q}_{\mathrm{AF}},\omega\to0}$ (see Fig. 3) being strongly increased over the mean-field behavior which determines the spin fluctuations at $\mathbf{q}=0$. Given the different T dependence for the spin-lattice relaxation rates for temperatures $T_N>T>T_{T_1}$ it is thus natural to identify this regime with the ASL physics.

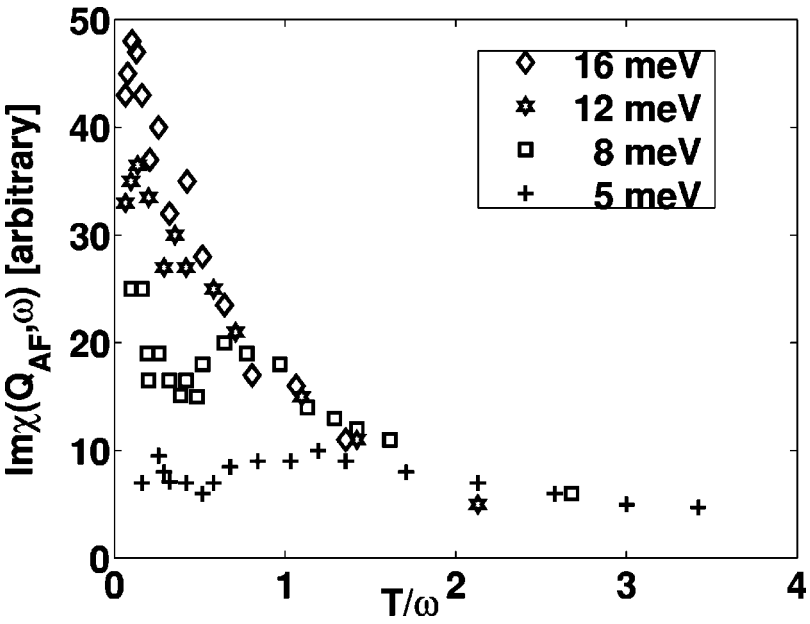

FIG. 9. Imaginary part of the spin susceptibility at $\mathbf{Q}_{\mathrm{AF}}$ taken from Sternlieb *et al*. Note the temperature dependence of the Imχ for a fixed ω converges to a universal function of T/ω at large T.

Sternlieb *et al.*[34] have performed temperature-dependent neutron scattering experiments on $YBa_2C_{u3}O_{6.6}$ ($T_c = 53$ K) and found a universal dependence of

$$\mathrm{Im}\chi(\omega) = \int \mathrm{Im}\chi(\mathbf{q},\omega)d\mathbf{q} \propto \mathrm{Im}\chi(\mathbf{Q}_{\mathrm{AF}},\omega) \tag{28}$$

on the ratio ω/T above a temperature $T \sim 100$ K. Their data (see Fig. 9) suggest that the temperature at which this universal scaling appears increases with decreasing energy. In particular for $\omega = 5$ meV the onset temperature is $T \sim 100$ K. Below this characteristic temperature (which again is well above T_c) their data show a decrease in spectrum which they associate with the opening of a spin pseudogap below $\omega_g \sim 10$ meV. They also point out that their data and the fact that the onset temperature of scaling increases with decreasing probe frequency are consistent with the anomalous behavior of $(1/T_1T)_{C_u}$ which probes $\omega \sim 0$ and increases down to $T = T_{T_1} \sim 150$ K.

As we argued above it is exactly the regime for $\omega > m$ at $T \sim 0$ or $T > T_m$ at $\omega \sim 0$ that we associate with the ASL physics. Under the assumption of perfect scaling we can thus account for the difference in $(1/T_1T)$ between C_u and O quite naturally. From

$$\frac{1}{T_1T} \propto \sum_{\mathbf{q}} \left.\frac{\mathrm{Im}\chi(\mathbf{q},\omega)}{\omega}\right|_{\omega\to 0}, \tag{29}$$

where, for C_u, $\Sigma_{\mathbf{q}} \sim \mathbf{Q}_{\mathrm{AF}}$ due to the form factor whereas O probes the uniform spin fluctuations. In the ASL we can for C_u approximate $\Sigma_{\mathbf{q}} \mathrm{Im}\chi(\mathbf{q},\omega)/\omega|_{\omega\to 0} \sim \mathrm{Im}\chi(\mathbf{Q}_{\mathrm{AF}},\omega)/\omega|_{\omega\to 0}$ which via scaling results in

$$\frac{1}{T_1T}(C_u) \propto \frac{1}{T^{2\nu}}, \quad 2\nu = \frac{32}{3\pi^2}, \tag{30}$$

whereas $(1/T_1T)_O$ falls monotonically as T is reduced following the uniform susceptibility (see Fig. 10). This is consistent with the temperature dependence seen by Sternlieb *et al.*, Fig. 9, at large T/ω.

The ASL gets destroyed below the mass gap energy scale which we associate with a temperature T_m. Below this temperature scale both the C_u and O spin-lattice relaxation rates fall monotonically following the sF-singlet correlations as T is reduced. This is seen in experiments (see Fig. 10).

Thus we associate the temperature $T_{T_1} \sim 150$ K where $(1/T_1T)_{C_u}$ shows the peak with T_m the temperature below which the massless U(1) gauge structure (and thus the underlying quantum order) becomes unstable and undergoes a ''transition'' (see the discussion at the end of this section)

To summarize the above comparison between the ASL and NMR experiments, we present the phase diagram, Fig. 11. Below the pseudogap scale T_{pg}, which we associate with T_N, the oxygen $1/T_1T$ starts to decrease due to the opening of the pseudogap associated with the spin-singlet formation.

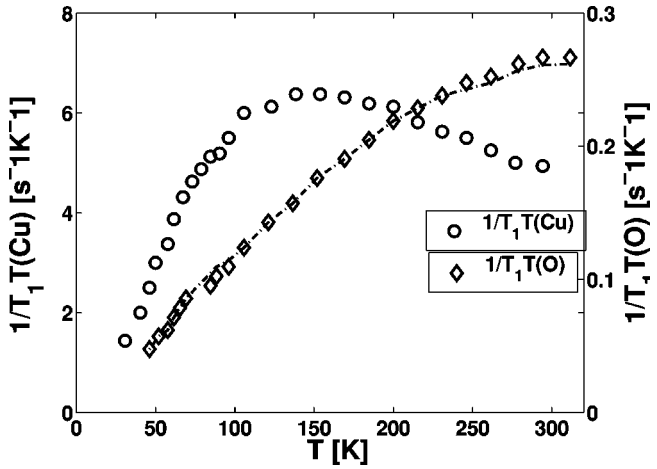

FIG. 10. Temperature dependence of $1/T_1T(C_u)$ and $1/T_1T(O)$ in $YBa_2C_{u3}O_{6.63}$. The dot-dashed line shows the temperature dependence of the static susceptibility. The data are taken from Ref. 35, which quotes Takigawa's results.

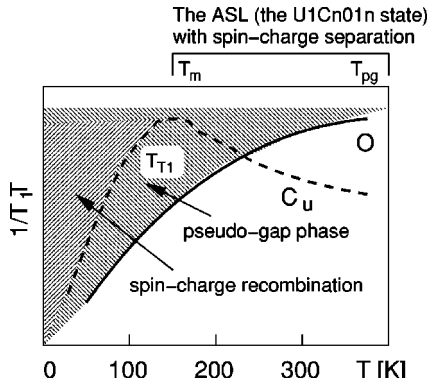

FIG. 11. Phase diagram implied by NMR experiments.

However, the copper $1/T_1T$ keeps increasing as temperature decreases, despite the small single-particle density of states in the pseudogap regime. This strange behavior can be explained very well by the ASL due to the diverging AF spin fluctuations at low energies even in the presence of the pseudogap. Below the temperature T_m, the U(1) gauge field starts to gain a gap and the enhancement in the AF spin fluctuations ceases to exist. This causes the copper $1/T_1T$ to decrease with decreasing temperature following the expected mean-field behavior. Thus the ASL described by the sF state (or the U1Cn01n state) appears between T_m (associated with the experimental temperature scale T_{T_1}) and T_{pg} (associated with the experimental scale T_N). Below T_m, the ASL will change into another state whose nature will be discussed later.

Let us now discuss the INS results which in their own right paint a very interesting picture of the spin fluctuations in the cuprates. First we consider the spectra at the antiferromagnetic ordering wave vector as a function of temperature and energy. Already well above the superconducting transition in the normal state, INS data show a marked increase in spectral weight at a finite characteristic frequency E_{spg} and a reduced spectral weight for $\omega < E_{spg}$ (the spin pseudogap; see Fig. 12 bottom curve, and compare Fig. 6).

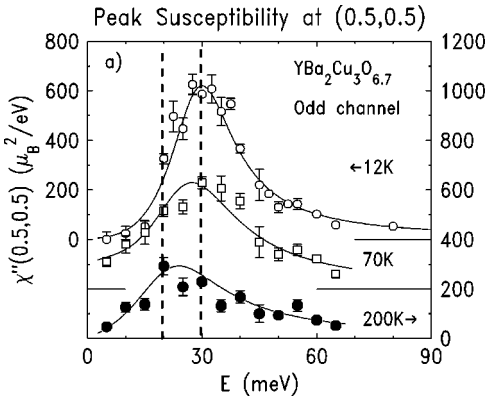

FIG. 12. Energy dependence of peak intensity at $\mathbf{Q}_{\mathrm{AF}}$ as a function of temperature taken from Fong *et al.* (Ref. 22). Note the shift in the peak position on decreasing the temperature below $T_c = 67$ K (the dashed lines were added by the current authors as a guide to the eye—see main text).

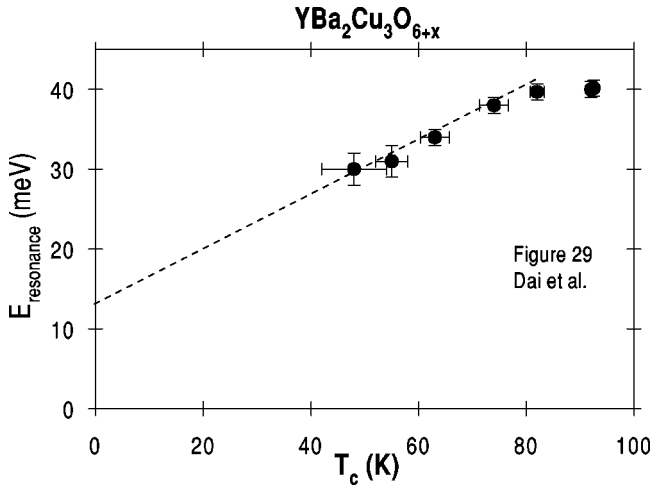

FIG. 13. The energy of the peak in the superconducting state—also called the *resonance* energy $E_{resonance}$ as a function of T_c in underdoped YBCO. Data taken from Dai *et al.* (Ref. 36). By extrapolating the linear relationship down to $T_c = 0$ (dashed line added as a guide) we extract an estimate for the mass scale related to topological gauge fluctuations.

On cooling below T_c this gap increases in size and the corresponding peak shifts to higher energies as depicted in Fig. 12 where we have added the two dashed lines to the data taken by Fong *et al.*[22] to guide the reader's eye. From the perspective of the ASL liquid the ''normal state'' above T_c corresponds to the phase where the gauge field is in the massive phase due to topological fluctuations. From the data by Dai *et al.*[36] see Fig. 13 we estimate the mass scale (i.e., the energy gap scale) due to instantons to be of the order of 10–15 meV which ties in nicely with the spin-pseudogap scale ~ 10 meV estimated by Sternlieb *et al.*

The shift of this peak to higher energies on cooling below T_c can be qualitatively understood as the contribution to the mass scale by condensed bosons via the Anderson-Higgs mechanism. This also explains the linear relationship between $E_{resonance}$ (where $E_{resonance}$ denotes the energy of the peak intensity in the superconducting state) and T_c (both being proportional to x, the hole doping concentration) as observed by Dai *et al.* in Fig. 13 for underdoped YBCO. Furthermore, we can account for the very different doping dependence of the normal-state maximum (determined by the instanton scale with weak doping dependence) versus the doping dependence of $E_{resonance}$ (determined by the condensed bosons $\propto x$) as was stressed in a recent article by Bourges.[37]

From this understanding of the ASL, we can conclude immediately that T_m, the temperature of the spin-pseudogap formation (and hence T_{T_1}), should be rather insensitive to changes in doping. Contrast this with the doping dependence of T_{pg}, the formation of the pseudogap in the single-particle spectrum which as $x \to 0$ will get as large as the spin-wave bandwidth, since in that limit the ASL will be described by the π-flux phase.

Another interesting point to discuss about the INS data is their momentum dependence. In Fig. 14 we show the data by Bourges taken on $YBa_2C_{u3}O_{6.5}(T_c = 52)$ which shows the

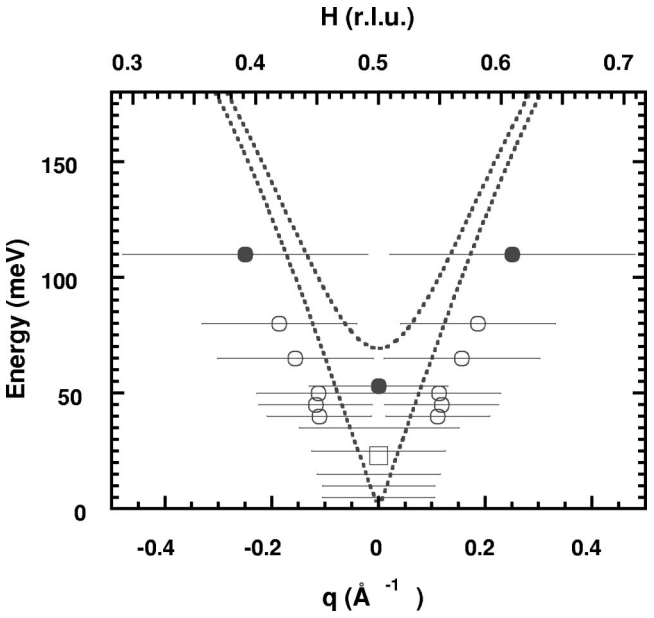

FIG. 14. Spin excitation spectrum for odd (open symbols) and even (solid circles) excitations at 5 K. The open square indicates the energy of the maximum of the odd susceptibility. The dotted lines correspond to the spin-wave dispersion relation in the insulating antiferromagnetic state with $J_{\parallel}=120$ meV. This figure is taken from Bourges *et al.* (Ref. 23).

spin-excitation spectrum for odd (acoustic) and even (optical) excitations at high energies. The dotted lines correspond to the spin-wave dispersion relation in the insulating antiferromagnetic state. The dispersive behavior compares nicely with Fig. 15 the correlations in the ASL liquid above the mass scale $m\sim 20$ meV.

So far we have argued for the strange phenomenology of the pseudogap phase to be tied to the physics embodied in the ASL. It is, however, clear that the ASL physics has to give way to the superconducting state at low temperatures. An important question is how this transition happens. Let us then briefly mention three plausible scenarios for how the ASL goes over to the superconducting state. In other words, we would like to understand how the U(1) gauge field gains a mass term which leads to the destruction of the ASL state.

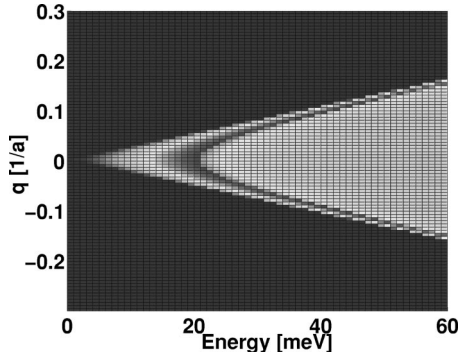

FIG. 15. Contour plot of Imχ—notice the ''spin pseudogap'' at $(q)=0\equiv\mathbf{Q}_{\mathrm{AF}}=(\pi/a,\pi/a)$ for energies below $m=20$ meV and the dispersion above m.

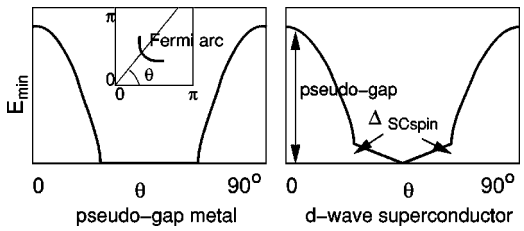

FIG. 16. Minimal quasiparticle energy E_{min} along the line in the θ direction. The left panel depicts the pseudogap metallic state and shows a finite Fermi arc. The right panel is for the superconducting state. In the superconducting state, the quasiparticle may have four bands (instead of the usual two for the BCS superconductor). For details, see Ref. 43.

In the first picture the mass of the U(1) gauge field is generated via confinement due to instantons. After the opening of the energy gap, there is no residual unbroken gauge structure left at low energies. Thus the confinement can also be referred to as U(1) gauge structure breaking down to Z_1. (Z_1 gauge structure means no gauge structure.) In the confinement phase [i.e., after the U(1) gauge field is gapped], the spinons and holons recombine into electrons which appear as the relevant degrees of freedom at low energies. Thus we also call the first picture spin-charge recombination. This in particular would suggest the existence of well-defined quasiparticles at low energies [as probed by angle-resolved photoemission spectroscopy (ARPES)] even above the superconducting transition temperature T_c (this should also be accompanied by T^2 resistance in dc conductivity). Furthermore, the binding of spinons and holons will gives rise to Fermi arcs.[10]

In the second picture, the U(1) gauge structure also breaks down to the Z_1 gauge structure, but now via holon condensation. In this case, $T_m=T_c$ and the ASL directly transforms into the *d*-wave superconducting state. There are no well-defined quasiparticles above T_c.

A third scenario might be the breaking of the U(1) gauge structure down to a Z_2 gauge structure via the condensation of spinon bilinear terms which do not break any symmetries.[38] (A Z_2 gauge structure was also found in a slave fermion description of spin systems via the condensation of boson bilinear terms which break 90° rotation symmetry.[39] The Z_2 gauge structure can also be obtained via the condensation of bound states of double vortices.[40]) The breaking from U(1) to Z_2 also results in a mass for the U(1) gauge field and leads to a new Z_2 spin liquid. The transition to this new topological and quantum order[38,4] implies the appearance of *true* spin-charge separation since the Z_2 gauge interaction is only short ranged[38–40] (Senthil experiment[41,42])

To determine which scenario actually applies to real high-T_c samples, we need to rely on experiments. In the following we would like to argue that experiments suggest the first scenario as most plausible in the high-T_c samples. The appearance of Fermi arcs in the first scenario implies a small energy scale Δ_{SCspin} for the spin excitations associated with the superconducting state (see Fig. 16). Such a small energy scale was observed in the experiment of Ref. 44 (see Fig. 17), where it was found that the spin susceptibility $\chi(\omega)$

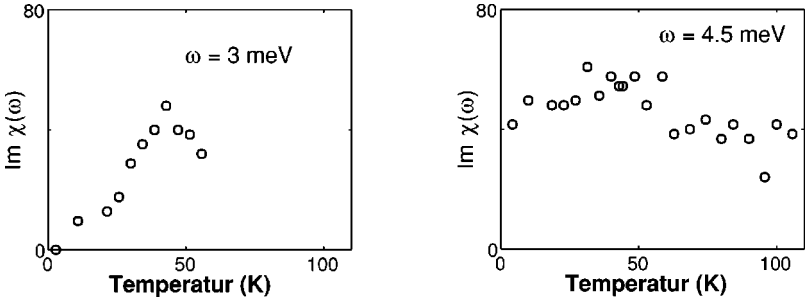

FIG. 17. Temperature evolution of $\chi(\mathbf{q},\omega)$ at the incommensurate peak position for energies of 3 meV and 4.5 meV. Data are taken from Yamada *et al.* (Ref. 44) whose sample was $La_{1.85}Sr_{0.15}C_uO_4(T_c=37.3\ \mathrm{K})$. Notice that the spectrum develops a gap for the 3 meV case on cooling below T_c.

decreases below T_c only when $\omega<4$ meV. This indicates that Δ_{SCspin} is as small as a few meV. Direct evidence for Fermi arcs comes from their observation in a recent photoemission experiment.[45] The expected well-defined electron-like quasiparticles near the Fermi arcs were also observed.

VII. CONCLUSION AND OPEN QUESTIONS

In this paper we have given an account of the spin correlations in the ASL phase through the calculation of $O(1/N)$ contributions depicted in Fig. 2. It was shown how the gauge fluctuations strongly enhance the staggered spin correlations, leaving the uniform spin correlation unaffected. This result is very natural within our effective gauge theory of underdoped samples where the uniform spin correlation is protected by current conservation and cannot have any anomalous dimension. From this perspective it is also easy to account for the qualitative different behaviors of planar C_u and O spin-lattice relaxation rates seen in NMR experiments where C_u probes the enhanced staggered correlations of the ASL down to a temperature scale $T_m\sim T_{T_1}$, where the C_u $1/(T_1T)$ peaks, which we associate with the appearance of an energy gap in the gauge spectrum. What is really remarkable in the ASL picture is that enhanced staggered spin correlations are obtained while at the same time having a small single-particle density of states within the pseudogap phase *without any fine-tuning*. As the doping x decreases, the pseudogap increases and, surprisingly, the staggered spin correlations also increase. This strange experimental behavior is explained naturally by the ASL picture.

It should be noted here that our ASL shows qualitative similarities with the quantum-critical-point scenario of Refs. 1 and 46. However, as was stressed in the paper,[46] the appearance of the pseudogap which they associate with the suppression of the spectral weight of spin waves characteristic of the quantum-disordered (QD) regime should affect the low-frequency dynamics for *both* $\mathbf{q}=0$ and $\mathbf{q}=(\pi,\pi)$. Within this framework it then seems hard to account for the qualitative different behaviors seen at the C_u and O sites in NMR experiments. As we have stressed many times, within the ASL, this difference is protected by the U(1) gauge structure. Also, in our ASL approach, we do not assume, in contrast to the quantum-critical-point approach, any nearby symmetry breaking phase and we do not require any strongly fluctuating order parameters to give us critical behavior. The ASL can by itself appear as a stable quantum phase or as a phase transition point between two states with new kinds of order—quantum order. The two states can have the *same symmetry* and no order parameters.[4] Hence the ASL associated with the transition between quantum orders can show scaling properties divorced from any critical point studied so far.

From this perspective the ASL is just one of a whole slew of possible quantum orders characterized by a massless U(1) gauge field coupled to massless Dirac fermions. It is also clear that the destruction of the ASL via the transition into a phase with a massive U(1) gauge field (phenomenologically described above via the introduction of the mass scale m) demands a much more careful analysis and highlights the main difficulty with the slave boson approach to the t-J model. Within this scheme it currently seems to be impossible or at least very challenging to describe this energy-temperature regime around m/T_m theoretically. The reason for that is related to the need of introducing a scale which is not tied to boson condensation and hence divorced from the mean-field energies and the corresponding degrees of freedom.

Through our examination of the experimental data, we find that the ASL, plus spin-charge recombination at lower energies, provides a consistent and natural (with no fine-tuning) description of underdoped cuprate superconductors. This is the main result and the bottom line of this paper.

ACKNOWLEDGMENTS

We would like to thank P. A. Lee and M. Kastner for many helpful discussions. W.R. would particularly like to thank A. Seidel for his mathematical insights and M. Reenders for pointing out Ref. 17. This work is supported by NSF Grant No. DMR-01-3156 and by NSF-MRSEC Grant No. DMR-98-08941.

APPENDIX A: SPIN OPERATORS IN THE CONTINUUM LIMIT

In this appendix we derive the expression for the spin operators near $\mathbf{q}=(0,0),(\pi,\pi)$, and $(\pi,0)$ in terms of the spinon field Ψ defined near the four nodes in momentum space:

Let us look at the staggered correlation in detail:

$$\vec{S}(\mathbf{Q}+\mathbf{q})=\frac{1}{2}\sum_{\mathbf{p}} f^{\dagger}(\mathbf{p}-\mathbf{q})\vec{\tau}f(\mathbf{p}+\mathbf{Q}), \tag{A1}$$

where $\mathbf{Q}=(\pi/a,\pi/a)$ and we have suppressed the frequency index. After introducing

$$f_e \equiv \frac{1}{\sqrt{2}}[f(\mathbf{q})+f(\mathbf{q}+\mathbf{Q})],$$
$$f_o \equiv \frac{1}{\sqrt{2}}[f(\mathbf{q})-f(\mathbf{q}+\mathbf{Q})], \tag{A2}$$

the expression for the staggered spin operator can be rewritten

$$\vec{S}(\mathbf{Q}+\mathbf{q})=\frac{1}{4}\sum_{\mathbf{p}}[f_e^\dagger(\mathbf{p}-\mathbf{q}),f_o^\dagger(\mathbf{p}-\mathbf{q})]\vec{\tau}(\sigma_3-i\sigma_2)\begin{pmatrix} f_e(\mathbf{p}) \\ f_o(\mathbf{p})\end{pmatrix}. \tag{A3}$$

Splitting the sum $\Sigma_{\mathbf{p}}=\Sigma_{\tilde{\mathbf{Q}}+\mathbf{k}}+\Sigma_{\tilde{\tilde{\mathbf{Q}}}+\mathbf{k}'}$ where $\tilde{\mathbf{Q}}=(\pi/2,\pi/2)$ and $\tilde{\tilde{\mathbf{Q}}}=(-\pi/2,-\pi/2)$ yields

$$\begin{aligned}\vec{S}(\mathbf{Q}+\mathbf{q})=&\frac{1}{4}\sum_{\mathbf{k}}[f_e^\dagger(\mathbf{k}-\mathbf{q}+\tilde{\mathbf{Q}}),f_o^\dagger(\mathbf{k}-\mathbf{q}+\tilde{\mathbf{Q}})]\\ &\times\vec{\tau}(\sigma_3-i\sigma_2)\begin{pmatrix} f_e(\mathbf{k}+\tilde{\mathbf{Q}}) \\ f_o(\mathbf{k}+\tilde{\mathbf{Q}})\end{pmatrix}\\ &+\frac{1}{4}\sum_{\mathbf{k}'}[f_e^\dagger(\mathbf{k}'-\mathbf{q}+\tilde{\tilde{\mathbf{Q}}}),f_o^\dagger(\mathbf{k}'-\mathbf{q}+\tilde{\tilde{\mathbf{Q}}})]\\ &\times\vec{\tau}(\sigma_3-i\sigma_2)\begin{pmatrix} f_e(\mathbf{k}'+\tilde{\tilde{\mathbf{Q}}}) \\ f_o(\mathbf{k}'+\tilde{\tilde{\mathbf{Q}}})\end{pmatrix}.\end{aligned} \tag{A4}$$

Noting $\tilde{\tilde{\mathbf{Q}}}=\tilde{\mathbf{Q}}+\mathbf{Q}$ and using $f_e(\mathbf{p}+\mathbf{Q})=f_e(\mathbf{p})$ and $f_o(\mathbf{p}+\mathbf{Q})=-f_o(\mathbf{p})$ we arrive at

$$\begin{aligned}\vec{S}(\mathbf{Q}+\mathbf{q})=&\frac{1}{2}\sum_{\mathbf{k}}[f_e^\dagger(\mathbf{k}-\mathbf{q}+\tilde{\mathbf{Q}}),f_o^\dagger(\mathbf{k}-\mathbf{q}+\tilde{\mathbf{Q}})]\\ &\times\vec{\tau}\sigma_3\begin{pmatrix} f_e(\mathbf{k}+\tilde{\mathbf{Q}}) \\ f_o(\mathbf{k}+\tilde{\mathbf{Q}})\end{pmatrix}\\ =&\frac{1}{2}\sum_{\mathbf{k}}\bar{\Psi}_1(\mathbf{k}-\mathbf{q})1\vec{\tau}\Psi_1(\mathbf{k}),\end{aligned} \tag{A5}$$

where $\bar{\Psi}_1(\mathbf{k}-\mathbf{q})=(f_e^\dagger(\mathbf{k}-\mathbf{q}+\tilde{\mathbf{Q}}),-f_o^\dagger(\mathbf{k}-\mathbf{q}+\tilde{\mathbf{Q}}))$ and $\mathbf{k}$ is measured away from the node of type $1\equiv\tilde{\mathbf{Q}}=\pm(\pi/2,\pi/2)$. The remaining contribution arises from the other two nodes in the spectrum at $\pm(\pi/2,-\pi/2)$.

Following the same calculation for the uniform correlation function

$$\vec{S}(\mathbf{q})=\frac{1}{2}\sum_{\mathbf{p}}f^\dagger(\mathbf{p}-\mathbf{q})\vec{\tau}f(\mathbf{p}), \tag{A6}$$

we find

$$\vec{S}(\mathbf{q})=\frac{1}{2}\sum_{\mathbf{k}}\bar{\Psi}_1(\mathbf{k}-\mathbf{q})\sigma_3\vec{\tau}\Psi_1(\mathbf{k}), \tag{A7}$$

with $\bar{\Psi}_1(\mathbf{k}-\mathbf{q})=(f_e^\dagger(\mathbf{k}-\mathbf{q}+\tilde{\mathbf{Q}}),-f_o^\dagger(\mathbf{k}-\mathbf{q}+\tilde{\mathbf{Q}}))$ and $\mathbf{k}$ is measured away from the node of type $1\equiv\tilde{\mathbf{Q}}=\pm(\pi/2,\pi/2)$. As before the remaining contribution arises from the other two nodes.

The correlation near $\mathbf{q}=(\pi,0)$ is obtained in a similar fashion the only difference here is that for this momentum transfer the two types of nodes get mixed and hence when we split up the sum over momentum space we need to consider all four nodes simultaneously. Under this proviso the calculation goes through as above and we end up with

$$\vec{S}(\mathbf{Q}_\mathbf{x}+\mathbf{q})=\frac{1}{2}\sum_{\mathbf{k}}\bar{\Psi}(\mathbf{k}-\mathbf{q})\begin{pmatrix} 0 & \sigma_1 \\ \sigma_1 & 0\end{pmatrix}\vec{\tau}\Psi(\mathbf{k}), \tag{A8}$$

where

$$\begin{aligned}\bar{\Psi}(\mathbf{k}-\mathbf{q})=[&f_e^\dagger(\mathbf{k}-\mathbf{q}+\mathbf{Q_1}),-f_o^\dagger(\mathbf{k}-\mathbf{q}+\mathbf{Q}_1),-f_o^\dagger(\mathbf{k}-\mathbf{q}\\ &+\mathbf{Q}_2),f_e^\dagger(\mathbf{k}-\mathbf{q}+\mathbf{Q}_2)],\end{aligned}$$

with $\mathbf{Q}_1=(\pi/2,\pi/2)$ and $\mathbf{Q}_2=(\pi/2,-\pi/2)$.

APPENDIX B: TWO-LOOP CALCULATION OF THE SPIN CORRELATION

We employ a four-dimensional representation of the Dirac algebra $\{\gamma_\mu,\gamma_\nu\}=2\delta_{\mu\nu}$ $(\mu,\nu=0,1,2)$ in the main body of the paper, i.e., $\mathrm{Tr}1=4$. To perform the Tr over the spinor indices we need the following identity:

$$\mathrm{Tr}[\gamma^\epsilon\gamma^\delta\gamma^\mu\gamma^\beta\gamma^\nu\gamma^\alpha]=\delta^{\alpha\nu}\mathrm{Tr}[\gamma^\epsilon\gamma^\delta\gamma^\mu\gamma^\beta]-\delta^{\alpha\beta}\mathrm{Tr}[\gamma^\epsilon\gamma^\delta\gamma^\mu\gamma^\nu]+\delta^{\alpha\mu}[\gamma^\epsilon\gamma^\delta\gamma^\beta\gamma^\nu]-\delta^{\alpha\delta}[\gamma^\epsilon\gamma^\mu\gamma^\beta\gamma^\nu]+\delta^{\alpha\epsilon}[\gamma^\delta\gamma^\mu\gamma^\beta\gamma^\nu],$$

which can be simply derived from the Dirac algebra by commuting γ matrices through and using the cyclic property of the trace Tr. Using the above identity we can simplify

$$[2(\mathrm{A})]=\int\frac{d^dk}{(2\pi)^d}\int\frac{d^dq}{(2\pi)^d}\mathrm{Tr}\left[\frac{8}{N}\frac{(p+k)_\epsilon\gamma^\epsilon k_\delta\gamma^\delta\gamma^\mu\gamma^\beta(k+q)_\beta\gamma^\nu\gamma^\alpha k_\alpha(\delta_{\mu\nu}\vec{q}^2-q_\mu q_\nu)}{(\vec{p}+\vec{k})^2\vec{k}^2(\vec{k}+\vec{q})^2\vec{k}^2|\vec{q}|^3}\right] \tag{B1}$$

to

$$[2(\mathrm{A})]=\frac{64}{N}\int\frac{d^dk}{(2\pi)^d}\int\frac{d^dq}{(2\pi)^d}\frac{[\vec{k}^2(\vec{p}+\vec{k})\cdot\vec{q}(\vec{k}+\vec{q})\cdot\vec{q}-2(\vec{p}+\vec{k})\cdot\vec{k}(\vec{k}+\vec{q})\cdot\vec{q}\vec{k}\cdot\vec{q}]}{(\vec{p}+\vec{k})^2(\vec{k}+\vec{q})^2\vec{k}^4\vec{q}^3} \tag{B2}$$

and for diagram [Fig. 2(C)] we obtain

$$[2(\mathrm{C})]=\int\frac{d^dk}{(2\pi)^d}\int\frac{d^dq}{(2\pi)^d}\mathrm{Tr}\left[\frac{8}{N}\frac{(p+k)_\epsilon\gamma^\epsilon\gamma^\mu(p+k+q)_\delta\gamma^\delta(k+q)_\beta\gamma^\beta\gamma^\nu k_\alpha\gamma^\alpha(\delta_{\mu\nu}\vec{q}^2-q_\mu q_\nu)}{(\vec{p}+\vec{k})^2(\vec{p}+\vec{k}+\vec{q})^2(\vec{k}+\vec{q})^2\vec{k}^2|\vec{q}|^3}\right] \tag{B3}$$

$$=\frac{64}{N}\int\frac{d^dk}{(2\pi)^d}\int\frac{d^dq}{(2\pi)^d}\frac{F(\vec{q},\vec{k},\vec{p})}{(\vec{p}+\vec{k})^2(\vec{p}+\vec{k}+\vec{q})^2(\vec{k}+\vec{q})^2\vec{k}^2|\vec{q}|^3}, \tag{B4}$$

where

$$F(\vec{q},\vec{k},\vec{p})=\left[\vec{k}^2\left(\vec{q}^2\vec{k}^2-\frac{1}{2}\vec{k}\cdot\vec{q}\vec{p}^2+2\vec{k}\cdot\vec{q}\vec{q}^2+\vec{k}\cdot\vec{p}\vec{q}\cdot\vec{p}-\frac{1}{4}\vec{q}^2\vec{p}^2+\vec{q}^4+(\vec{q}\cdot\vec{p})^2\right)+\frac{1}{2}(\vec{k}+\vec{q})^2\left(2\vec{q}^2\vec{k}\cdot\vec{p}+\vec{p}^2\vec{k}\cdot\vec{q}-2\vec{k}\cdot\vec{p}\vec{q}\cdot\vec{p}\right.\right.$$
$$\left.\left.-\frac{1}{2}\vec{q}^2\vec{p}^2\right)+(\vec{k}+\vec{p})^2\left(\vec{q}^2\vec{p}\cdot\vec{q}+\vec{q}^2\vec{k}\cdot\vec{p}-\frac{1}{2}\vec{q}^2\vec{p}^2\right)+\frac{1}{4}\vec{q}^4\vec{p}^2-\vec{p}^2\vec{q}^2\vec{q}\cdot\vec{p}+\frac{1}{2}\vec{q}^2\vec{p}^4\right].$$

In both expressions (B2) and (B3) the integration over $\vec{k}$ is convergent in $d=3$ and can be performed noting that

$$\int\frac{d^3k}{(2\pi)^3}\frac{1}{\vec{k}^2(\vec{k}+\vec{p})^2(\vec{k}+\vec{q})^2}=\frac{1}{8|\vec{p}||\vec{q}||\vec{q}-\vec{p}|}, \tag{B5}$$

$$\int\frac{d^3k}{(2\pi)^3}\frac{1}{\vec{k}^2(\vec{k}+\vec{p})^2(\vec{k}+\vec{q})^2(\vec{k}+\vec{p}+\vec{q})^2}$$
$$=\frac{1}{8|\vec{q}||\vec{p}|\vec{q}\cdot\vec{p}}\left[\frac{1}{|\vec{p}-\vec{q}|}-\frac{1}{|\vec{q}+\vec{p}|}\right]. \tag{B6}$$

Thus after the $\vec{k}$ integration we arrive at

$$[2(\mathrm{A})]=\frac{2}{N}\int\frac{d^dq}{(2\pi)^d}\left[\frac{2\vec{p}\cdot\vec{q}+\vec{p}^2}{|\vec{q}|^3|\vec{p}+\vec{q}|}-\frac{\vec{p}\cdot\vec{q}}{|\vec{p}|\vec{q}^2|\vec{p}+\vec{q}|}-\frac{|\vec{p}|}{|\vec{q}|^3}\right], \tag{B7}$$

$$[2(\mathrm{C})]=\frac{4}{N}\int\frac{d^dq}{(2\pi)^d}\left[\frac{2}{\vec{q}^2}+\frac{|\vec{p}|}{|\vec{q}|^3}-\frac{\vec{p}^2+2\vec{p}\cdot\vec{q}}{|\vec{q}|^3|\vec{p}+\vec{q}|}-\frac{4|\vec{p}|}{\vec{q}^2|\vec{p}+\vec{q}|}\right.$$
$$\left.-\frac{\vec{q}^2\vec{p}^2+2\vec{p}^4}{\vec{p}\cdot\vec{q}\vec{q}^2|\vec{p}||\vec{p}+\vec{q}|}\right]. \tag{B8}$$

Adding the contributions

$$2\times[2(\mathrm{A})]+[2(\mathrm{C})]=\frac{4}{N}\int\frac{d^dq}{(2\pi)^d}\left[\frac{2}{\vec{q}^2}-\frac{4|\vec{p}|}{\vec{q}^2|\vec{p}+\vec{q}|}\right.$$
$$\left.-\frac{\vec{p}\cdot\vec{q}}{|\vec{p}|\vec{q}^2|\vec{p}+\vec{q}|}-\frac{\vec{q}^2\vec{p}^2+2\vec{p}^4}{\vec{p}\cdot\vec{q}\vec{q}^2|\vec{p}||\vec{p}+\vec{q}|}\right]. \tag{B9}$$

As noted previously, because of the $\vec{p}\cdot\vec{q}$ term in the denominator of the last term above, we wont use dimensional regularization. Therefore we set $d=3$ and introduce an upper cutoff Λ to regularize the above integrals. Also note that we will neglect the first term in Eq. (B9) which is linearly divergent whose appearance is tight to the regularization via a momentum cutoff (such divergences do not appear in Lorentz invariant regularization schemes).

Under this proviso we obtain the following result for the last three terms in Eq. (B9):

$$\frac{4}{N}\left[-\frac{8|\vec{p}|}{4\pi^2}-\frac{4|\vec{p}|}{4\pi^2}\ln\frac{\Lambda^2}{\vec{p}^2}+\frac{2|\vec{p}|}{36\pi^2}+\frac{|\vec{p}|}{12\pi^2}\ln\frac{\Lambda^2}{\vec{p}^2}\right.$$
$$\left.+\frac{|\vec{p}|}{8\pi^2}(C_1+C_2)+\frac{2|\vec{p}|}{8\pi^2}\ln\frac{\Lambda^2}{\vec{p}^2}\right], \tag{B10}$$

where the last term (B9) is given by

$$\int\frac{d^3q}{(2\pi)^3}\frac{\vec{q}^2\vec{p}^2+2\vec{p}^4}{\vec{p}\cdot\vec{q}\vec{q}^2|\vec{p}||\vec{p}+\vec{q}|}$$
$$=\frac{|\vec{p}|}{8\pi^2}\left[\int_0^1dy\frac{2+y}{y\sqrt{1+y}}\ln\frac{\sqrt{1+y}-\sqrt{y}}{\sqrt{1+y}+\sqrt{y}}\right.$$
$$\left.+\int_1^{\Lambda^2/\vec{p}^2}dy\frac{2+y}{y\sqrt{1+y}}\ln\frac{\sqrt{1+y}-1}{\sqrt{1+y}+1}\right] \tag{B11}$$

$$=-\frac{|\vec{p}|}{8\pi^2}\left(C_1+C_2+2\ln\frac{\Lambda^2}{\vec{p}^2}\right) \tag{B12}$$

and

$$C_1 = -\int_0^1 dy \frac{2+y}{y\sqrt{1+y}} \ln \frac{\sqrt{1+y}-\sqrt{y}}{\sqrt{1+y}+\sqrt{y}} = 7.748128723,$$

$$C_2 = 4\ln(\sqrt{2}-1) + 4 + \ln(3-2\sqrt{2})^2 - 2\ln(3-2\sqrt{2}) + 2\ln(3-2\sqrt{2})\sqrt{2} = 2.121475665.$$

Finally extracting the logarithmically divergent terms we arrive at the result stated in the body of the text.

APPENDIX C: ANALYTIC CONTINUATION OF 1/*N* CORRECTION

Having obtained the $1/N$ correction we would now like to reexponentiate our result in the form

$$\langle S_s^+(\vec{q}) S_s^-(\vec{q})\rangle_0 = -\frac{\sqrt{\vec{q}^2}}{16} - \frac{8}{12\pi^2 N}\sqrt{\vec{q}^2}\ln\left(\frac{\Lambda^2}{\vec{q}^2}\right) \sim -\frac{\Lambda^{2\nu}}{16}(q^2)^{1/2-\nu}, \quad \nu = \frac{32}{3\pi^2 N}. \tag{C1}$$

This however immediately confronts us with the problem that after analytically continuing Eq. (C1) the susceptibility has the wrong sign for $2\nu > 1$. It is, however, hard to understand why the spin operator cannot have an anomalous dimension bigger than $\frac{1}{2}$. In order to analyze this issue it is helpful to look at the corresponding Euclidean real space correlations. Let us take the case of a general staggered spin correlation of the form

$$\langle S_s^+(\vec{x}) S_s^-(0)\rangle = \frac{1}{16\pi^2}(-1)^{\mathbf{x}} \frac{C}{|\vec{x}|^{4-2\nu}}, \tag{C2}$$

where the spin operator has anomalous dimension ν. We now Fourier transform this to obtain

$$\frac{1}{4\pi}|\vec{q}|^{1-2\nu}\int_0^\infty \frac{du}{u^{3-2\nu}}\sin(u). \tag{C3}$$

For $0 < |\mathrm{Re}(2\nu-2)| < 1$ this can be evaluated[47] to give

$$\frac{1}{4\pi}\Gamma(2\nu-2)\sin[(\nu-1)\pi]|\vec{q}|^{1-2\nu}. \tag{C4}$$

This leads after analytic continuation to the result, Eq. (16). From here it is easy to see how the Γ function and the sine function which are missed in the naive exponentiation of the Euclidean momentum space result conspire to give the correct sign for the spin correlation no matter what the size of the anomalous dimension. In particular we can continue the above for the case $\nu \to 0$ to give the correct mean-field result.

APPENDIX D: TWO-LOOP CALCULATION IN THE MASSIVE PHASE OF THE U(1) GAUGE FIELD

This appendix gives some details of the calculation leading to the $O(1/N)$ corrections to the staggered spin correlation in the case when the gauge field is in the massive phase with propagator

$$D_{\mu\nu}(\vec{q}) = \frac{8}{N\sqrt{\vec{q}^2+m^2}}\left(\delta_{\mu\nu} - \frac{q_\mu q_\nu}{\vec{q}^2}\right).$$

We can use the results derived in Appendix A for the integrals over $\vec{k}$, Eq. (B9), since they are unaffected by the change in the gauge propagator:

$$2[2(\mathrm{A})]+[2(\mathrm{C})] = \frac{4}{N}\int \frac{d^dq}{(2\pi)^d}\left[-\frac{4|\vec{p}|}{|\vec{q}|\sqrt{\vec{q}^2+m^2}|\vec{p}+\vec{q}|} - \frac{\vec{p}\cdot\vec{q}}{|\vec{p}||\vec{q}|\sqrt{\vec{q}^2+m^2}|\vec{p}+\vec{q}|} - \frac{\vec{q}^2\vec{p}^2+2\vec{p}^4}{\vec{p}\cdot\vec{q}|\vec{q}|\sqrt{\vec{q}^2+m^2}|\vec{p}||\vec{p}+\vec{q}|}\right], \tag{D1}$$

where we have neglected the linearly divergent term as discussed above. After integration over $\vec{q}$ in $d=3$ we arrive at

$$\frac{4}{N}\Bigg[-\frac{2}{\pi^2}[\sqrt{\vec{p}^2+m^2}-m] - \frac{2|\vec{p}|}{\pi^2}\ln\frac{2\Lambda}{|\vec{p}|+\sqrt{\vec{p}^2+m^2}} + \frac{\sqrt{\vec{p}^2+m^2}}{6\pi^2} - \frac{1}{9\pi^2\vec{p}^2}[(\vec{p}^2+m^2)^{3/2}-m^3] + \frac{|\vec{p}|}{6\pi^2}\ln\frac{2\Lambda}{|\vec{p}|+\sqrt{\vec{p}^2+m^2}} - \frac{|\vec{p}|}{8\pi^2}\int_0^1 dy \frac{2+y}{\sqrt{y}\sqrt{y+\left(\frac{m}{|\vec{p}|}\right)^2}\sqrt{1+y}}\ln\frac{\sqrt{1+y}-\sqrt{y}}{\sqrt{1+y}+\sqrt{y}} - \frac{|\vec{p}|}{8\pi^2}\int_1^{\Lambda^2/\vec{p}^2} dy \frac{2+y}{\sqrt{y}\sqrt{y+\left(\frac{m}{|\vec{p}|}\right)^2}\sqrt{1+y}}\ln\frac{\sqrt{1+y}-1}{\sqrt{1+y}+1}\Bigg]. \tag{D2}$$

It is not hard to check that in the limit $|\vec{p}|/m \to 0$ the terms proportional to m cancel. In extracting the logarithmic term we have to take a closer look at the last term which cannot be

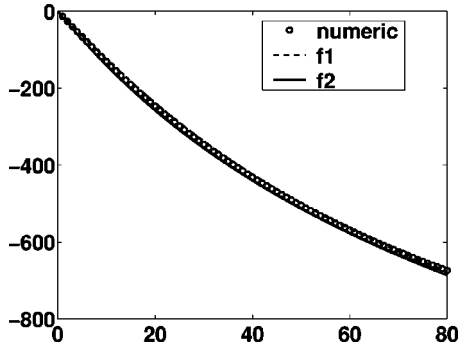

FIG. 18. Comparison between $f1=-2|\vec{p}|\ln[\Lambda^2/(\vec{p}^2+m^2)]$, $f2=-4|\vec{p}|\ln[2\Lambda/(|\vec{p}|+\sqrt{\vec{p}^2+m^2})]$, and the numeric evaluation of Eq. (D3) before analytic continuation ($m=30$).

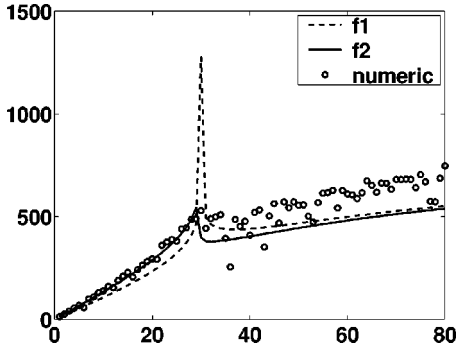

FIG. 19. Comparison between the analytically continued forms of $f1$, $f2$ and the numeric evaluation of Eq. (D3) after analytic continuation ($m=30$).

evaluated in a closed form. In Fig. 18 we compare two different functional forms with the numeric evaluation of

$$|\vec{p}|\int_1^{\Lambda^2/\vec{p}^2} dy \frac{2+y}{\sqrt{y}\sqrt{y+\left(\frac{m}{|\vec{p}|}\right)^2}\sqrt{1+y}} \ln\frac{\sqrt{1+y}-1}{\sqrt{1+y}+1}. \tag{D3}$$

Note that there is virtually no difference between $f1=-2|\vec{p}|\ln[\Lambda^2/(\vec{p}^2+m^2)]$ and $f2=-4|\vec{p}|\ln[2\Lambda/(|\vec{p}|+\sqrt{\vec{p}^2+m^2})]$. However, this comparison has to be taken with a grain of salt as we are still in Euclidean space but are interested in the analytically continued forms. In Fig. 19 we plot the analytically continued ($ip_0\rightarrow\omega+i\epsilon$) forms of the above functions. From this comparison it is now obvious that $f1$ which has developed a pole at m is unsuitable as an approximation and we take $f2$ which fits the numerically integrated form quite well. Collecting the logarithmic-terms in Eq. (D2) we obtain

$$2\times[2(\mathrm{A})]_m+[2(\mathrm{C})]_m=-\frac{16|\vec{q}|}{3\pi^2 N}\ln\frac{2\Lambda}{|\vec{q}|+\sqrt{\vec{q}^2+m^2}}. \tag{D4}$$

Analytically continuing and combining with the mean-field result (10) gives Eq. (22).

APPENDIX E: LOW-ENERGY EFFECTIVE THEORY FOR THE SUPERCONDUCTING STATE

Starting from the mean-field Hamiltonian for the spinons,

$$H=\frac{1}{2}\sum_{i,j,\sigma}\psi^\dagger_{\sigma i}\tilde{J}U_{ij}\psi_{\sigma j}+\sum_{il}a^l_{0i}\frac{1}{2}\psi^\dagger_{\sigma i}\tau^l\psi_{\sigma i}, \tag{E1}$$

in the d-wave paired state

$$U_{i,i+\hat{x}}=-\tau^3\chi+\tau^1\Delta,$$

$$U_{i,i+\hat{y}}=-\tau^3\chi-\tau^1\Delta,$$

$$a^3_0\neq 0, \tag{E2}$$

we obtain after Fourier transformation the following Lagrangian:

$$L=\sum_{\mathbf{q},\omega}[f^\dagger_\uparrow(\mathbf{q},\omega),f_\downarrow(-\mathbf{q},-\omega)]\begin{pmatrix}-i\omega+\epsilon(\mathbf{q})+a^3_0 & -\eta(\mathbf{q})\\ -\eta(\mathbf{q}) & -i\omega-\epsilon(\mathbf{q})-a^3_0\end{pmatrix}\begin{pmatrix}f_\uparrow(\mathbf{q},\omega)\\ f^\dagger_\downarrow(-\mathbf{q},-\omega)\end{pmatrix}, \tag{E3}$$

$$\epsilon(\mathbf{q})=-2\tilde{J}\chi[\cos(q_xa)+\cos(q_ya)],\quad \eta(\mathbf{q})=-2\tilde{J}\Delta[\cos(q_xa)-\cos(q_ya)], \tag{E4}$$

which results, with

$$S^+(\mathbf{q},\omega)=\frac{1}{2}\sum_{\mathbf{k},\omega_k}f^\dagger_\uparrow(\mathbf{k},\omega_k)f_\downarrow(\mathbf{k}+\mathbf{q},\omega_k+\omega_q),$$

$$S^-(\mathbf{q},\omega)=\frac{1}{2}\sum_{\mathbf{k},\omega_k}f^\dagger_\downarrow(\mathbf{k},\omega_k)f_\uparrow(\mathbf{k}+\mathbf{q},\omega_k+\omega_q), \tag{E5}$$

in

$$\langle S^+(\mathbf{q},\omega)S^-(-\mathbf{q},-\omega)\rangle=\frac{1}{4}\sum_{\mathbf{k},\omega_k}\frac{[-i\omega_k-\epsilon(\mathbf{k})-a_0^3][i\omega_k-i\omega_q+\epsilon(\mathbf{k}-\mathbf{q})+a_0^3]-\eta(\mathbf{k})\,\eta(\mathbf{k}-\mathbf{q})}{\{\omega_k^2+[\epsilon(\mathbf{k})+a_0^3]^2+\eta(\mathbf{k})^2\}\{(\omega_k-\omega_q)^2+[\epsilon(\mathbf{k}-\mathbf{q})+a_0^3]^2+\eta(\mathbf{k}-\mathbf{q})^2\}}. \tag{E6}$$

Next, we split $\Sigma_{\mathbf{k}}=\Sigma_{\mathbf{Q}_i+\tilde{p}}$ where $\mathbf{Q}_i$ with $i=1,\ldots,4$ corresponds to $(\pi/2,\pi/2),(-\pi/2,-\pi/2),(\pi/2,-\pi/2),(-\pi/2,\pi/2)$ in this order. To extract the correlations near $\mathbf{Q}_{\mathrm{AF}}=(\pi,\pi)$ we write $\mathbf{q}=\mathbf{Q}_{\mathrm{AF}}+\tilde{k}$.

Concentrating on one of the terms in the sum—e.g., about $\mathbf{Q}_1=(\pi/2,\pi/2)$ we can expand

$$\epsilon(\mathbf{Q}_1+\tilde{p})\sim v_f p_1,\quad \eta(\mathbf{Q}_1+\tilde{p})\sim -v_2 p_2,\quad v_f\equiv 2\sqrt{2}\chi J,\quad v_2\equiv 2\sqrt{2}\delta J,\quad p_1\equiv\frac{\tilde{p}_x+\tilde{p}_y}{\sqrt{2}},\quad p_2\equiv\frac{-\tilde{p}_x+\tilde{p}_y}{\sqrt{2}} \tag{E7}$$

to obtain

$$\langle S^+(\mathbf{Q}_{\mathrm{AF}}+\tilde{\mathbf{k}},\omega)S^-(-\mathbf{Q}_{\mathrm{AF}}-\tilde{\mathbf{k}},-\omega)\rangle$$
$$=\frac{1}{4}\sum_{\mathbf{Q}_1,\omega_p}\frac{(-i\omega_p-v_f p_1-a_0^3)(i\omega_p-i\omega_k-v_f(p_1-k_1)+a_0^3)+v_2 p_2 v_2(p_2-k_2)}{[\omega_p^2+(v_f p_1+a_0^3)^2+v_2^2p_2^2]\{(\omega_p-\omega_k)^2+[-v_f(p_1-k_1)+a_0^3]^2+v_2^2(p_2-k_2)^2\}}+\frac{1}{4}\sum_{\mathbf{Q}_i,\omega_p,i=2,\ldots,4}\cdots. \tag{E8}$$

Note that $k_1\equiv(\tilde{k}_x+\tilde{k}_y)/\sqrt{2}$ and $k_2\equiv(-\tilde{k}_x+\tilde{k}_y)/\sqrt{2}$. Now we approximate the sums by integrals and define

$$\overline{p_1}\equiv v_f p_1+a_0^3,\quad \overline{p_2}\equiv v_2 p_2,$$
$$\overline{k_1}\equiv v_f k_1+2a_0^3,\quad \overline{k_2}\equiv v_2 k_2,$$

which allows us to rewrite the first term in Eq. (E8)

$$\frac{1}{4}\int\frac{d^3\overline{p}}{(2\pi)^3 v_f v_2}\frac{\vec{\overline{p}}\cdot(\vec{\overline{p}}-\vec{\overline{k}})+i\overline{p_1}\omega_k-i\omega_p\overline{k_1}}{[\vec{\overline{p}}^2(\vec{\overline{p}}-\vec{\overline{k}})^2]}. \tag{E9}$$

Using the Feynman trick or otherwise it is not hard to convince oneself that the last two terms cancel each other and the final result is

$$-\frac{1}{64 v_f v_2}\sqrt{\omega_k^2+\overline{k_1^2}+\overline{k_2^2}}. \tag{E10}$$

Combining all four contributions from the four nodes in this way and translating the $\overline{k}$'s back to the $\tilde{k}$'s which measure momentum along the ab axis away from $\mathbf{Q}_{\mathrm{AF}}$ we obtain after analytic continuation

$$\mathrm{Im}\langle S^+(\omega,\mathbf{Q}_{\mathrm{AF}}+\tilde{\mathbf{k}})S^-(-\omega,-\mathbf{Q}_{\mathrm{AF}}-\tilde{\mathbf{k}})\rangle=\frac{1}{64 v_f v_2}\{\theta[\omega^2-(v_f k_1+2a_0^3)^2-v_2^2k_2^2]\sqrt{\omega^2-(v_f k_1+2a_0^3)^2-v_2^2k_2^2}$$
$$+\theta[\omega^2-(v_f k_1-2a_0^3)^2-v_2^2k_2^2]\sqrt{\omega^2-(v_f k_1-2a_0^3)^2-v_2^2k_2^2}$$
$$+\theta[\omega^2-(v_f k_2+2a_0^3)^2-v_2^2k_1^2]\sqrt{\omega^2-(v_f k_2+2a_0^3)^2-v_2^2k_1^2}$$
$$+\theta[\omega^2-(v_f k_2-2a_0^3)^2-v_2^2k_1^2]\sqrt{\omega^2-(v_f k_2-2a_0^3)^2-v_2^2k_1^2}\},$$
$$k_1\equiv\frac{\tilde{k}_x+\tilde{k}_y}{\sqrt{2}},\quad k_2\equiv\frac{-\tilde{k}_x+\tilde{k}_y}{\sqrt{2}},\quad v_f\equiv 2\sqrt{2}aJ\chi,\quad v_2\equiv 2\sqrt{2}aJ\Delta, \tag{E11}$$

the result stated in the main body of the paper.

[1] A.V. Chubukov, S. Sachdev, and J. Ye, Phys. Rev. B **49**, 11 919 (1994).
[2] A. Sokol and D. Pines, Phys. Rev. Lett. **71**, 2813 (1993); V. Barzykin, D. Pines, A. Sokol, and D. Thelen, Phys. Rev. B **49**, 1544 (1994).
[3] Xiao-Gang Wen, Phys. Rev. Lett. **88**, 011602 (2002).
[4] Xiao-Gang Wen, Phys. Rev. B **65**, 165113 (2002); Phys. Rev. B **65**, 165113 (2002).

[5] P.W. Anderson, Science **235**, 1196 (1987).
[6] Ian Affleck and J. Brad Marston, Phys. Rev. B **37**, 3774 (1988).
[7] G. Kotliar, Phys. Rev. B **37**, 3664 (1988); G. Kotliar and J. Liu, Phys. Rev. B **38**, 5142 (1988).
[8] D.H. Kim and P.A. Lee, Ann. Phys. (N.Y.) **272**, 130 (1999).
[9] J.B. Marston and I. Affleck, Phys. Rev. B **39**, 11 538 (1989).
[10] X.G. Wen and P.A. Lee, Phys. Rev. Lett. **76**, 503 (1996).
[11] W. Rantner and Xiao-Gang Wen, Phys. Rev. Lett. **86**, 3871 (2001).
[12] G. Baskaran and P.W. Anderson, Phys. Rev. B **37**, 580 (1988); L.B. Ioffe and A.I. Larkin, *ibid.* **39**, 8988 (1989); P. Lee and N. Nagaosa, *ibid.* **46**, 5621 (1992); G. Baskaran, Z. Zou, and P.W. Anderson, Solid State Commun. **63**, 973 (1987).
[13] I. Affleck, Z. Zou, T. Hsu, and P.W. Anderson, Phys. Rev. B **38**, 745 (1988); X.G. Wen and P.A. Lee, Phys. Rev. Lett. **76**, 503 (1996).
[14] P.A. Lee, N. Nagaosa, T.K. Ng, and X.-G. Wen, Phys. Rev. B **57**, 6003 (1998); J.B. Marston and I. Affleck *ibid.* **39**, 11 538 (1989).
[15] W. Chen, M.P.A. Fisher, and Y.S. Wu, Phys. Rev. B **48**, 13 749 (1993).
[16] D.A. Ivanov, P.A. Lee, and X.-G. Wen, Phys. Rev. Lett. **84**, 3958 (2000).
[17] V. Gusynin, A. Hams, and M. Reenders, Phys. Rev. D **63**, 045025 (2001).
[18] L.B. Ioffe and A.I. Larkin, Phys. Rev. B **39**, 8988 (1989).
[19] H. Yoshizawa, S. Mitsuda, H. Kitazawa, and K. Katsumata, J. Phys. Soc. Jpn. **57**, 3686 (1988).
[20] R.J. Birgeneau, Y. Endoh, K. Kakurai, Y. Hidaka, T. Murakami, M.A. Kastner, T.R. Thurston, G. Shirane, and K. Yamada, Phys. Rev. B **39**, 2868 (1989).
[21] S.-W. Cheong, G. Aeppli, T.E. Mason, H. Mook, S.M. Hayden, P.C. Canfield, Z. Fisk, K.N. Clausen, and J.L. Martinez, Phys. Rev. Lett. **67**, 1791 (1991).
[22] H.F. Fong, B. Keimer, D.L. Milius, and I.A. Aksay, Phys. Rev. Lett. **78**, 713 (1997).
[23] P. Bourges H.F. Fong, L.P. Regnault, J. Bossy, C. Vettier, D.L. Milius, I.A. Aksay, and B. Keimer, Phys. Rev. B **56**, 11 439 (1997).
[24] K. Yamada, C.H. Lee, K. Kurahashil, J. Wada, S. Wadimoto, S. Ueki, H. Kimura, U. Endoh, S. Hosoya, G. Shirane, R.J. Birgeneau, M. Greven, M.A. Kastner, and Y.J. Kim, Phys. Rev. B **57**, 6165 (1998).
[25] H. Fong, P. Bourges, Y. Sidis, L.P. Regnault, J. Bossy, A. Ivanov, D.L. Milius, I.A. Aksay, and B. Keimer, Phys. Rev. B **61**, 14 773 (2000).
[26] M. Ubbens and P.A. Lee, Phys. Rev. B **46**, 8434 (1992).
[27] J. Brinckmann and P.A. Lee, Phys. Rev. Lett. **82**, 2915 (1999); Ying-Jer Kao, Qimiao Si, and K. Levin, Phys. Rev. B **61**, R11 898 (2000).
[28] H.A. Mook, Pengcheng Dai, S.M. Hayden, G. Aeppli, T.G. Perring, and F. Dogan, Nature (London) **395**, 580 (1998).
[29] M. Arai, T. Nishijima, Y. Endoh, T. Egami, S. Tajima, K. Tomimoto, Y. Shiohara, M. Takahashi, A. Garrett, and S.M. Bennington, Phys. Rev. Lett. **83**, 608 (1999)
[30] K. Krishana, N.P. Ong, Y. Zhang, Z.A. Xu, R. Gagnon, and L. Taillefer, Phys. Rev. Lett. **82**, 5108 (1999).
[31] J. Rossat-Mignod, L. P. Regnault, C. Vettier, P. Bourges, P. Burlet, J. Bossy, J. Y. Henry, and G. Lapertot, Physica C **86**, 185 (1991).
[32] Ph. Bourges, in *The Gap Symmetry and Fluctuations in High Temperature Superconductors*, Vol. 371 of *NATO Advanced Study Institute, Series B: Physics*, edited by J. Bok, G. Deutscher, D. Pavuna, and S.A. Wolf (Plenum, 1998), pp. 349–379.
[33] T. Tanamoto, H. Kohno, and H. Fukuyama, J. Phys. Soc. Jpn. **63**, 2739 (1994).
[34] B.J. Sternlieb, G. Shirane, J.M. Tranquad, M. Sato, and S. Shamoto, Phys. Rev. B **47**, 5320 (1993).
[35] C.P. Slichter, in *Strongly Correlated Electronic Materials*, The Los Alamos Symposium 1993, edited by Bedell, Wang, Meltzer, Balatsky, and Abrahams (Addison-Wesley, Reading, MA, 1994).
[36] Pengcheng Dai, H.A. Mook, R.D. Hunt, and F. Dogan, Phys. Rev. B **63**, 054525 (2001).
[37] Ph. Bourges, in *Neutron Scattering in Novel Materials, Proceedings of the 8th PSI Summer School on Neutron Scattering, Zuoz, Switzerland*, edited by A. Furrer (World Scientific, Singapore, 2000).
[38] Xiao-Gang Wen, Phys. Rev. B **44**, 2664 (1991).
[39] N. Read and Subir Sachdev, Phys. Rev. Lett. **66**, 1773 (1991).
[40] L. Balents, M.P.A. Fisher, and C. Nayak, Int. J. Mod. Phys. B **12**, 1033 (1998).
[41] T. Senthil and M.P.A. Fisher, Phys. Rev. Lett. **86**, 292 (2001).
[42] D.A. Bonn, Janice C. Wynn, Brian W. Gardner, Yu-Ju Lin, Ruixing Liang, W.N. Hardy, J.R. Kirtley, and K.A. Moler, Nature (London) **414**, 887 (2001).
[43] Patrick A. Lee and Xiao-Gang Wen, Phys. Rev. Lett. **78**, 4111 (1997).
[44] K. Yamada, S. Wakimoto, G. Shirane, C.H. Lee, M.A. Kastner, S. Hosoya, M. Greven, Y. Endoh, and R.J. Birgeneau, Phys. Rev. Lett. **75**, 1626 (1995).
[45] Z. X. Shen (private communication).
[46] V. Barzykin, D. Pines, A. Sokol, and D. Thelen, Phys. Rev. B **49**, 1544 (1994).
[47] I. S. Gradshteyn and I. M. Ryzhik, *Table of Integrals, Series, and Products*, 5th ed. (Academic, San Diego, CA, 1994).